WP15ER-PR(17) 17107

F Deluzet et al.

Iterative solvers for elliptic problems with arbitrary anisotropy strengths.

Preprint of Paper to be submitted for publication in
Multiscale Modeling and Simulation

This work has been carried out within the framework of the EUROfusion Consortium and has received funding from the Euratom research and training programme 2014-2018 under grant agreement No 633053. The views and opinions expressed herein do not necessarily reflect those of the European Commission.

Iterative solvers for elliptic problems with arbitrary anisotropy strengths.

C. Yang[†], J. Claustre[‡], F. Deluzet[‡*]

January 25, 2017

Abstract

This paper is devoted to the introduction of iterative methods for the Asymptotic-Preserving (AP) resolution of anisotropic elliptic problems arising in magnetized plasma simulation. The methods investigated in this paper extend the precedent realizations, limited to the finite element framework, to finite difference discretizations. They also overcome the resolution of a Saddle point problem for which only sparse direct solvers have been successfully operated so far. Although very efficient for two dimensional computations, the cost of direct methods is considerable for real scale three dimensional problems hardly addressed in precedent achievements. This difficulty receives an appropriate answer in this paper, the new methods providing system matrices with a condition number uniformly bounded with respect to the anisotropy strength without the resolution of a Saddle point problem. An iterative resolution of the AP scheme is developed, offering a numerical cost comparable to the resolution of isotropic elliptic problems. This brings a leap forward in the computational efficiency of the method, conclusively outlined thanks to three dimensional serial computations carrying out tens of millions of unknowns.

1 Introduction

This paper is devoted to the construction of iterative methods for the numerical resolution of anisotropic elliptic equations which prototype writes

$$-\nabla_\perp \cdot \Big(A_\perp \nabla_\perp \phi\Big) - \frac{1}{\varepsilon}\nabla_\parallel \cdot \Big(A_\parallel \nabla_\parallel \phi\Big) = f\,, \qquad \text{in } \Omega\,, \tag{1a}$$

$$n \cdot \nabla_\parallel \phi = 0\,, \quad \text{on } \partial\Omega_\parallel\,, \tag{1b}$$

$$\phi = 0\,, \quad \text{on } \partial\Omega_\perp\,. \tag{1c}$$

The parallel and perpendicular directions relate to a vector b, assumed to be the normalized magnetic field B in the framework of plasma physics, $b = B/\|B\|$. In this paper the geometry

*Corresponding author

will be simplified and the magnetic field will be assumed to be straight and aligned to the z-direction (x, y and z being the Cartesian coordinates), with $\nabla_\parallel = (0, 0, \partial_z)^T$, $\nabla_\perp = (\partial_x, \partial_y, 0)^T$. More complex anisotropy topologies may be addressed thanks to dedicated coordinate systems widely used for plasma modelling (see the references in [16]). In the system (1) $A_\perp$ and $A_\parallel$ are positive functions of the space variables $(x, y, z) \in \Omega$. The domain boundary is decomposed into $\partial\Omega = \partial\Omega_\parallel \cup \partial\Omega_\perp$, the anisotropy direction being perpendicular to the outward normal n on $\Omega_\perp$, yielding to $b(s) \cdot n(s) = 0\,, \forall s \in \partial\Omega_\perp$. Note that the Neumann boundary conditions considered at the magnetic field line ends, *ie* on $\partial\Omega_\parallel$, can be substituted by periodic ones to cope with the torus geometry of tokamak. The asymptotic parameter ε parameterizes the strength of the anisotropy.

This kind of equations is common in the context of plasma simulation under large magnetic fields, good example of which being ionospheric or tokamak plasmas. In particular, this equation is verified by the electric potential in quasi-neutral fluid descriptions of the ionospheric plasma (see [5, 27, 22, 8]) and tokamak plasma modelling [3]. It may also describe the anisotropic diffusion of the temperature [20, 29, 13], the density or the pressure [11, 10, 14, 19] in plasmas evolving under large magnetic fields. For these applications, the anisotropy strength ε^{-1} has large values, the maximum values ranging from 10^7 to 10^{10} (see [26, appendix B], [23, 34]) for aniospheric plasmas, the objectived being $\varepsilon^{-1} > 10^6$ for the tokamak simulations investigated in [21, 30]. In these applications, the physics of interest is that of the perpendicular directions. Therefore an efficient numerical method should be able to follow the transverse evolution without any constraints on the numerical parameter related to the fast parallel dynamic. This problem is challenging from a numerical point of view. Indeed, in the limit of an infinite anisotropy, the dominant operator (carried by ε^{-1}) does not define a well posed problem, due to the Neumann boundary conditions it is supplemented with. Therefore, standard numerical methods give rise to a system matrix with a bad conditionning number for large anisotropies and fail to provide an accurate approximation of the solution. The convergence of the solver is reported to fail for $\varepsilon^{-1} > 10^4$ in [30], while the numerical investigations are limited to moderate anisotropies ($\varepsilon < 10^3$) in [13] and eventually performed with a refinement of the numerical parameters to offset the anisotropy increase [20, 13].

Asymptotic-Preserving (AP) schemes have proved to be free from these constraints, providing a system matrix with a conditioning independent of the anisotropy [18, 29, 12] (see also [24] for seminal work on AP-methods and [25, 14, 15] for reviews). The pros of these approaches is the possibility to handle arbitrary values for ε and to choose the discretization parameters according to the physic of interest rather than the asymptotic parameter values. The cons of the existing realizations lie in the reformulation of the equation into a Saddle point problem. Though the system matrix exhibits good properties with respect to the condition number, standard iterative methods usually efficient for elliptic problems are inoperative for the AP formulations. To date, all the realizations proposed rely on a resolution of the system matrix by means of direct solvers and are limited to two dimensional frameworks. Although, very efficient for two dimensional problems, direct solvers become too much resource demanding for three dimensional simulations on refined meshes. This explains why

AP methods have not been used so far for three dimensional realistic simulations.

Another bottleneck to the generalization of the use of these methods can be explaind by the fact that they are limited to the finite element framework. While this formalism is well suited for the analyze of Saddle point problems, it is quite cumbersome for the discretization of the conservation laws to which the anisotropic equations are coupled in order to evolve the other quantities describing the plasma.

These are the issues addressed in this paper. The first goal of the present work is to provide new AP formulations derived from the Duality-Based decomposition [18, 8] that secure the same AP property but without the resolution of the Saddle point problem of the precedent realizations. A rigorous analysis is conducted to demonstrate that the system matrices issued from these AP reformulations have a condition number uniformly bounded with respect to the anisotropy strength. The new formulations introduced here allow for the resolution by preconditioned Krylov (or multigrid methods) available in classical scientific libraries. Although the first goal of the AP methods is to derive system matrices with good conditioning, this is the first time this linear systems are solved by iterative methods and take advantage of this property. The gains in term of efficiency compared to the sparse direct solvers used so far are substantial for three dimensional computations, making possible to tackle three dimensional simulations with tens of millions of unknowns on a sequential computer, a task that remained totally out of reach thanks to precedent achievements. The second goal is to provide a discretization of the AP formulation in the frame of finite difference methods which are more in line with the numerical methods routinely implemented for the conservation laws coupled to the anisotropic equation.

The singular nature of the problem (1) is first recalled in Sec 2. The outlines of the duality based method are then precised and new AP formulations are introduced. These approaches avoid the introduction of a Saddle point problem and are discretized in the finite difference framework. The iterative solver strategy is finally defined. The properties of these schemes are investigated in Sec. 3, in particular we demonstrate that the AP formulations share the interesting properties of the precedent achievements. The considerable gains in the efficiency are then demonstrated thanks to three dimensional computations with an application to ionospheric plasma simulation.

2 An elliptic problem characteristic of magnetized plasma simulations

2.1 The issue raised by the model problem

Let us simplify the problem to a two dimensional configuration assuming that the quantities only depend on the aligned coordinate z and one transverse coordinate x, yielding the

Singular Perturbation problem

$$\text{(SP)}\quad \begin{cases} -\dfrac{\partial}{\partial x}\left(A_\perp \dfrac{\partial \phi^\varepsilon}{\partial x}\right) - \dfrac{1}{\varepsilon}\dfrac{\partial}{\partial z}\left(A_\parallel \dfrac{\partial \phi^\varepsilon}{\partial z}\right) = f^\varepsilon\,, \quad \text{in } [0, L_x]\times[0, L_z]\,, & \text{(2a)} \\ \dfrac{\partial \phi^\varepsilon}{\partial z} = 0\,, \quad \text{for } z \in \{0, L_z\}\,, & \text{(2b)} \\ \phi^\varepsilon = 0\,, \quad \text{for } x \in \{0, L_x\}\,. & \text{(2c)} \end{cases}$$

Multiplying Eq. (2a) by ε and letting formally $\varepsilon \to 0$ yields the *Degenerate* problem

$$\text{(D)}\quad \begin{cases} -\dfrac{\partial}{\partial z}\left(A_\parallel \dfrac{\partial \phi^0}{\partial z}\right) = 0\,, \quad \text{in } [0, L_x]\times[0, L_z]\,, \\ \dfrac{\partial \phi^0}{\partial z} = 0\,, \quad z \in \{0, L_z\}\,, \\ \phi^0 = 0\,, \quad x \in \{0, L_x\}\,. \end{cases} \tag{3}$$

This set of equations is ill posed. It is reduced to an operator whose kernel contains all the functions that do not depend on the aligned coordinate z. However, this shows that, in the limit, the solution of the problem is a function of the only coordinate x (see [17]). A well posed problem for ϕ^0 can be recovered by integrating the equation (2a) along the anisotropy direction. This yields to the following definition of the *Limit* problem

$$\text{(L)}\quad \begin{cases} \dfrac{\partial}{\partial x}\left(\bar{A}_\perp \dfrac{\partial \phi^0}{\partial x}\right) = \bar{f}^0\,, \quad \text{in } [0, L_x]\,, & \text{(4a)} \\ \phi^0 = 0\,, \quad x \in \{0, L_x\}\,, \end{cases}$$

with the mean value $\bar{f}$ of a function defined as

$$\bar{f}(x) = \frac{1}{L_z}\int_0^{L_z} f(x, z)\, dz\,. \tag{4b}$$

The purpose of AP schemes is to capture this limit system (4) preventing by this means the degeneracy of the problem for vanishing ε.

2.2 Asymptotic preserving methods in the finite difference framework

The starting point of these investigations consists of the Duality Based reformulation introduced in [17] and reworked in [16, 8]. The outline are recalled in the next lines and we refer to these references for the details. The Duality Based reformulation operates a decomposition of the functions into a mean value along the anisotropy direction corrected by a fluctuating part accordingly to

$$\phi(x, z) = \bar{\phi}(x) + \phi'(x, z)\,, \quad \forall (x, z) \in [0, L_x]\times[0, L_z]\,, \qquad \text{with } \bar{\phi}' = 0\,.$$

This ansatz is inserted into the system (2) to provide a set of coupled equations providing the two components of the solution, thanks to

$$\begin{cases} -\dfrac{\partial}{\partial x}\left(\bar{A}_\perp \dfrac{\partial \bar{\phi}}{\partial x}\right) = \bar{f} + \dfrac{\partial}{\partial x}\left(\overline{A_\perp \dfrac{\partial \phi'}{\partial x}}\right) , \quad \text{in } [0, L_x],, \\ \bar{\phi} = 0 , \quad x \in \{0, L_x\} , \end{cases} \tag{5a}$$

$$\begin{cases} -\varepsilon \dfrac{\partial}{\partial x}\left(A_\perp \dfrac{\partial \phi'}{\partial x}\right) - \dfrac{\partial}{\partial z}\left(A_\parallel \dfrac{\partial \phi'}{\partial z}\right) = \varepsilon f + \varepsilon \dfrac{\partial}{\partial x}\left(A_\perp \dfrac{\partial \bar{\phi}}{\partial x}\right) , \text{ in } [0, L_x] \times [0, L_z] , \\ \partial_z \phi' = 0 , \quad z \in \{0, L_z\} , \\ \phi' = 0 , \quad x \in \{0, L_x\} , \\ \overline{\phi'} = 0 , \quad \text{in } [0, L_x] . \end{cases} \tag{5b}$$

Note that in the limit $\varepsilon \to 0$ the degenerated problem (3) is recovered from the equation (5b). However this system is satisfied by the fluctuation ϕ' with a zero mean constraint which restores the well posedness of the system regardless to ε. The unique solution of the system (5b) in the limit $\varepsilon \to 0$ is $\phi' = 0$, which inserted into (5a) yields to the limit problem (4). This demonstrates, that in the reformulated system (5), the limit $\varepsilon \to 0$ is a regular perturbation.

An asymptotic Preserving method is obtained by a standard discretization of this reformulated system. Since this set of equations unifies the two regimes with a smooth transition to the well posed limit problem, the condition number of the matrix should not deteriorate with vanishing ε. This property is conclusively demonstrated by the preceding realizations [18, 16, 8]. The main difficulty to overcome in deriving the numerical scheme lies in the discretization of the fluctuation zero mean constraint supplementing the equation (5b). In the precedent achievements, a weak formulation is introduced along with a finite element method. Since the discretization of a functional space with zero mean value functions is not straightforward, this property is penalized thanks to the introduction of a Lagrangian multiplier λ. The system in thus turned into is a Saddle point problem for (ϕ', λ) avoided by the discretization introduced here.

The new fomulation of the AP system relies on the property that one of the boundary conditions used at the magnetic field line extremities is already included in the system.

Proposition 2.1. *The system providing the fluctuation ϕ' can be equivalently stated as*

$$\begin{cases} -\varepsilon \dfrac{\partial}{\partial x}\left(A_\perp \dfrac{\partial \phi'}{\partial x}\right) - \dfrac{\partial}{\partial z}\left(A_\parallel \dfrac{\partial \phi'}{\partial z}\right) = \varepsilon f + \varepsilon \dfrac{\partial}{\partial x}\left(A_\perp \dfrac{\partial \bar{\phi}}{\partial x}\right) , \ \textit{in } [0, L_x] \times [0, L_z] , & \text{(6a)} \\ \dfrac{\partial \phi'}{\partial z} = 0 , \quad \textit{on } z = 0 , & \text{(6b)} \\ \phi' = 0 , \quad x \in \{0, L_x\} , & \text{(6c)} \\ \overline{\phi'} = 0 , \quad \textit{in } [0, L_x] . & \text{(6d)} \end{cases}$$

Proof. Computing the mean of the equation (6a) we get

$$-\frac{1}{L_z}\left[A_\parallel \frac{\partial \phi'}{\partial z}\right]_{z=0}^{z=L_z} = \varepsilon \left(\bar{f} + \frac{\partial}{\partial x}\left(\bar{A}_\perp \frac{\partial \bar{\phi}}{\partial x}\right) + \frac{\partial}{\partial x}\left(\overline{A_\perp \frac{\partial \phi'}{\partial x}}\right)\right) .$$

Thanks to (5a), the right hand side of this equation vanishes. On the other hand, the homogeneous Neumann boundary condition (6b) implies that $\partial_z \phi'|_{z=N_z} = 0$. □

Another AP formulation may be proposed as stated in the following proposition.

Proposition 2.2. *The problem* (2) *can be equivalently reformulated into*

$$\begin{cases} -\dfrac{\partial}{\partial x}\left(\bar{A}_\perp \dfrac{\partial p}{\partial x}\right) = \bar{f} + \dfrac{\partial}{\partial x}\left(\overline{A_\perp \dfrac{\partial q}{\partial x}}\right), \quad in\ [0, L_x], \\ p = 0, \quad x \in \{0, L_x\}, \end{cases} \tag{7a}$$

$$\begin{cases} -\varepsilon \dfrac{\partial}{\partial x}\left(A_\perp \dfrac{\partial q}{\partial x}\right) - \dfrac{\partial}{\partial z}\left(A_\parallel \dfrac{\partial q}{\partial z}\right) = \varepsilon f + \varepsilon \dfrac{\partial}{\partial x}\left(A_\perp \dfrac{\partial p}{\partial x}\right), \ in\ [0, L_x] \times [0, L_z], \\ q = 0, \qquad x \in \{0, L_x\}, \\ q = 0, \qquad on\ z = 0, \\ \dfrac{\partial q}{\partial z} = 0, \qquad on\ z = L_z; \end{cases} \tag{7b}$$

with

$$\phi(x, z) = p(x) + q(x, z). \tag{7c}$$

We wish to point out that a similar idea is developed in a very recent work [33] implementing a mean of the equation along the magnetic field lines in substitution of one of the boundary conditions at one magnetic field ends. This integrated equation bare some analogies with the equation providing the mean component of the solution in (5). This offers the advantage to avoid the decomposition of the solution and to solve a system with two unknowns. However, the system matrix obtained by this means is much more filled with non zeros elements. Indeed, after discretization, the stencil of the discrete operator involves at least five unknowns for two dimensional computations, nine for three dimensional problems. This may be increased for higher methods with wider stencils. In the approach proposed here, the only unknowns carried by a field line are involved in the mean constraint which reduces significantly the fill in of the system matrix. Moreover, one of the component of the solution is two dimensional which amounts to a cost related to the computation of this part completely offset by that of the three dimensional component. The resolution of a three dimensional elliptic problem is much more resources demanding than a two dimensional one, hence the importance to reduce the cost as much as possible of the three dimensional system resolution. This will be outlined further by the numerical investigations proposed in the sequel.

The decomposition (7c) shares some analogies with the micro-macro decomposition (see for instance [28, 29]) however the re-scaling of q is not implemented here and the reformulation of the system is also completely different.

Remark 2.1. *For non-homogeneous anisotropies, the system* (6) *is recast into*

$$\begin{cases} -\dfrac{\partial}{\partial x}\left(A_\perp \dfrac{\partial \phi'}{\partial x}\right) - \dfrac{\partial}{\partial z}\left(\dfrac{A_\parallel}{\varepsilon}\dfrac{\partial \phi'}{\partial z}\right) = f + \dfrac{\partial}{\partial x}\left(A_\perp \dfrac{\partial \bar{\phi}}{\partial x}\right)\,, \ \textit{in } [0, L_x]\times[0, L_z]\,, \\ \partial_z \phi' = 0\,, \quad z \in \{0, L_z\}\,, \\ \phi' = 0\,, \qquad x \in \{0, L_x\}\,, \\ \overline{\phi'} = 0\,, \qquad \textit{in } [0, L_x]\,. \end{cases} \tag{8}$$

Now, let us consider a monotonic asymptotic parameter, for instance a non-increasing function, with very strong variations along the z-coordinate, i.e.

$$\varepsilon(0) \gg \varepsilon(L_z).$$

Integrating the fluctuation equation along z and by using the mean equation, we obtain

$$-\frac{A_\parallel}{\varepsilon}\frac{\partial \phi'}{\partial z}\bigg|_{z=L_z} + \frac{A_\parallel}{\varepsilon}\frac{\partial \phi'}{\partial z}\bigg|_{z=0} = 0\,.$$

For large variations of ε, due to the computer finite precision arithmetic, this equation degenerate into

$$-\frac{A_\parallel}{\varepsilon}\frac{\partial \phi'}{\partial z}\bigg|_{z=L_z} = 0.$$

This means the choice of the boundary condition substituted by the well posedness condition (either the zero mean constraint or the Dirichlet boundary condition) should be made with care. The asymptotic preserving property is preserved by keeping the Neumann condition on the boundary where the anisotropy is the weakest (largest value of ε).

2.3 A finite difference space discretization

The Cartesian mesh is defined by the nodes at position (x_i, z_k) with

$$x_i = (i - 1/2)\Delta x\,, \quad z_k = (k - 1/2)\Delta z\,, \quad \forall (i,k) \in [1, \mathrm{N_x}]\times[1, \mathrm{N_z}]\,,$$

and $\Delta x = L_x/(\mathrm{N_x} - 2)$, $\Delta z = L_z/(\mathrm{N_z} - 2)$. Let $\Phi'_h = ((\phi'_h)_{i,k})$ be the vector containing $(\phi'_h)_{i,k}$ the approximation of $\phi'(x_i, z_k)$ for $(i,k) \in [1, \mathrm{N_x}]\times[1, \mathrm{N_z}]$ and $\bar{\Phi}_h = (\bar{\phi}_h)_i$ with $(\bar{\phi}_h)_i \approx \bar{\phi}(x_i)$, $i \in [1, \mathrm{N_x}]$. The discrete projector onto the mean functions is defined for any vector $(\Phi_h) = (\phi_h)_{i,k}$ as

$$\Pi_h(\Phi_h)_i = \frac{1}{L_z}\sum_{k=2}^{\mathrm{N_z}-1} \Delta z\,(\phi_h)_{i,k}\,. \tag{9}$$

Finally, we introduce the bijection I: $(i,k) \in [1, \mathrm{N_x}]\times[1, \mathrm{N_z}] \to I(i,k) \in [1, \mathrm{N_x}\cdot\mathrm{N_z}]$. This numerotation will be defined in the next sections. With these notations, the discrete operators can be defined.

Definition 2.1. *We denote* $\bar{\mathcal{A}}_\perp$ *and* $\mathcal{A}_\perp$ *the* $\mathbb{R}^{\mathrm{N_x}\times\mathrm{N_x}}$ *and* $\mathbb{R}^{(\mathrm{N_x}\mathrm{N_z})\times(\mathrm{N_x})}$ *matrices defined as*

$$\big(\bar{\mathcal{A}}_\perp\bar{\Phi}_h\big)_i = \begin{cases} \dfrac{1}{2}\Big((\bar{\phi}_h)_i + (\bar{\phi}_h)_{i+1}\Big) & i = 1\,, \\ \dfrac{(\bar{A}_\perp)_{i+1/2}}{\Delta x}(\partial_x^h\bar{\Phi}_h)_{i+1/2} - \dfrac{(\bar{A}_\perp)_{i-1/2}}{\Delta x}(\partial_x^h\bar{\Phi}_h)_{i-1/2}\,, & i \in [2, \mathrm{N_x}-1]\,, \\ \dfrac{1}{2}\Big((\bar{\phi}_h)_{i-1} + (\bar{\phi}_h)_i\Big) & i = \mathrm{N_x}\,; \end{cases} \tag{10a}$$

$$\big(\mathcal{A}_\perp\bar{\Phi}_h\big)_{I(i,k)} = \begin{cases} 0 & i \in \{1, \mathrm{N_x}\}, \\ \dfrac{(A_\perp)_{i+1/2,k}}{\Delta x}(\partial_x^h\bar{\Phi}_h)_{i+1/2} & \\ \qquad - \dfrac{(A_\perp)_{i-1/2,k}}{\Delta x}(\partial_x^h\bar{\Phi}_h)_{i-1/2}\,, & (i,k) \in [2, \mathrm{N_x}-1]\times[1,\mathrm{N_z}]\,; \end{cases} \tag{10b}$$

with

$$(\partial_x^h\bar{\Phi}_h)_{i+1/2} = \frac{1}{\Delta x}\Big((\bar{\phi}_h)_{i+1} - (\bar{\phi}_h)_i\Big)\,. \tag{10c}$$

A similar definition is proposed for the discrete operators applied to the component of the solution with non vanishing aligned gradient.

Definition 2.2. *We denote by* $\bar{\mathbb{A}}_\perp \in \mathbb{R}^{(\mathrm{N_x})\times(\mathrm{N_x}\mathrm{N_z})}$, $\mathbb{A}_\perp \in \mathbb{R}^{(\mathrm{N_x}\mathrm{N_z})\times(\mathrm{N_x}\mathrm{N_z})}$ *and* $\mathbb{A}_\parallel \in \mathbb{R}^{(\mathrm{N_x}\mathrm{N_z})\times(\mathrm{N_x}\mathrm{N_z})}$ *the matrices verifying*

$$\big(\bar{\mathbb{A}}_\perp\Phi_h'\big)_i = \begin{cases} 0\,, & i \in \{1, \mathrm{N_x}\}\,, \\ \big(\Pi_h(\Psi_h)\big)_i\,, & i \in [2, \mathrm{N_x}-1]\,; \end{cases} \tag{11a}$$

where $\Psi_h = (\psi_h)_{i,k}$ *is the vector defined by*

$$(\psi_h)_{i,k} = \frac{(A_\perp)_{i+1/2,k}}{\Delta x}(\partial_x^h\Phi_h')_{i+1/2,k} - \frac{(A_\perp)_{i-1/2,k}}{\Delta x}(\partial_x^h\Phi_h')_{i-1/2,k}\,, \quad (i,k) \in [2,\mathrm{N_x}-1]\times[1,\mathrm{N_z}]\,;$$

$$(\mathbb{A}_\perp\Phi_h')_{I(i,k)} = \begin{cases} \dfrac{1}{2}\Big((\phi_h')_{i,k} + (\phi_h')_{i+1,k}\Big)\,, & (i,k) \in \{1\}\times[1,\mathrm{N_z}]\,, \\ \dfrac{(A_\perp)_{i+1/2,k}}{\Delta x}(\partial_x^h\phi_h')_{i+1/2,k} & \\ \qquad - \dfrac{(A_\perp)_{i-1/2,k}}{\Delta x}(\partial_x^h\phi_h')_{i-1/2,k}\,, & (i,k) \in [2,\mathrm{N_x}-1]\times[1,\mathrm{N_z}]\,, \\ \dfrac{1}{2}\Big((\phi_h')_{i-1,k} + (\phi_h')_{i,k}\Big)\,, & (i,k) \in \{\mathrm{N_x}\}\times[1,\mathrm{N_z}]\,, \end{cases} \tag{11b}$$

$$\big(\mathbb{A}_\parallel\Phi_h'\big)_{I(i,k)} = \begin{cases} (\partial_z^h\phi_h')_{i,k+1/2}\,, & (i,k) \in [2,\mathrm{N_x}-1]\times\{1\}\,, \\ (\partial_z^h\phi_h')_{i,k-1/2}\,, & (i,k) \in [2,\mathrm{N_x}-1]\times\{\mathrm{N_z}\}\,, \\ 0\,, & (i,k) \in \{1,\mathrm{N_x}\}\times[1,\mathrm{N_z}]\,, \\ \dfrac{(A_\parallel)_{i,k+1/2}}{\Delta z}(\partial_z^h\phi_h')_{i,k+1/2} & \\ \qquad - \dfrac{(A_\parallel)_{i,k-1/2}}{\Delta z}(\partial_z^h\phi_h')_{i,k-1/2}\,, & (i,k) \in [2,\mathrm{N_x}-1]\times[2,\mathrm{N_z}-1]\,; \end{cases} \tag{11c}$$

$$\left(\mathbb{A}_{\parallel}^{M}\Phi'_h\right)_{I(i,k)} = \begin{cases} (\partial_z^h \phi'_h)_{i,k+1/2}\,, & (i,k) \in [2, \mathrm{N_x}-1] \times \{1\}\,, \\ \left(\Pi_h(\Phi'_h)\right)_i\,, & (i,k) \in [2, \mathrm{N_x}-1] \times \{\mathrm{N_z}\}\,, \\ 0\,, & (i,k) \in \{1, \mathrm{N_x}\} \times [1, \mathrm{N_z}]\,, \\ \dfrac{(A_{\parallel})_{i,k+1/2}}{\Delta z}(\partial_z^h \phi'_h)_{i,k+1/2} & \\ \quad - \dfrac{(A_{\parallel})_{i,k-1/2}}{\Delta z}(\partial_z^h \phi'_h)_{i,k-1/2}\,, & (i,k) \in [2, \mathrm{N_x}-1] \times [2, \mathrm{N_z}-1]\,; \end{cases} \tag{11d}$$

$$\left(\mathbb{A}_{\parallel}^{D}\Phi'_h\right)_{I(i,k)} = \begin{cases} (\partial_z^h \phi'_h)_{i,k+1/2}\,, & (i,k) \in [2, \mathrm{N_x}-1] \times \{1\}\,, \\ \dfrac{1}{2}\Big((\Phi'_h)_{i,k-1} + (\Phi'_h)_{i,k}\Big)\,, & (i,k) \in [2, \mathrm{N_x}-1] \times \{\mathrm{N_z}\}\,, \\ 0\,, & (i,k) \in \{1, \mathrm{N_x}\} \times [1, \mathrm{N_z}]\,, \\ \dfrac{(A_{\parallel})_{i,k+1/2}}{\Delta z}(\partial_z^h \phi'_h)_{i,k+1/2} & \\ \quad - \dfrac{(A_{\parallel})_{i,k-1/2}}{\Delta z}(\partial_z^h \phi'_h)_{i,k-1/2}\,, & (i,k) \in [2, \mathrm{N_x}-1] \times [2, \mathrm{N_z}-1]\,; \end{cases} \tag{11e}$$

with

$$\begin{aligned} (\partial_x^h \Phi'_h)_{i+1/2,k} &= \frac{1}{\Delta x}\Big((\phi'_h)_{i+1,k} - (\phi'_h)_{i,k}\Big)\,, \\ (\partial_z^h \Phi'_h)_{i,k+1/2} &= \frac{1}{\Delta z}\Big((\phi'_h)_{i,k+1} - (\phi'_h)_{i,k}\Big)\,. \end{aligned} \tag{11f}$$

With these definitions we can state the finite differenced system with a discrete analog of the proposition 2.1

Proposition 2.3. *Using the definitions 2.1 and 2.2, the set of equations (5a–6) and* (7) *are discretized by the linear system*

$$\begin{pmatrix} \bar{\mathcal{A}}_{\perp} & \bar{\mathbb{A}}_{\perp} \\ \varepsilon\mathcal{A}_{\perp} & \varepsilon\mathbb{A}_{\perp} + \mathbb{A}_{\parallel}^{\alpha} \end{pmatrix} \begin{pmatrix} \bar{\Phi}_h \\ \Phi'_h \end{pmatrix} = \begin{pmatrix} \bar{F}_h \\ \varepsilon F_h \end{pmatrix} \tag{12a}$$

where $\mathbb{A}_{\parallel}^{\alpha}$ *stands for* $\mathbb{A}_{\parallel}^{M}$ *or* $\mathbb{A}_{\parallel}^{D}$*, and*

$$(F_h)_{I(i,k)} = \begin{cases} 0\,, & i \in \{1, \mathrm{N_x}\} \text{ or } k = N_z\,, \\ f(x_i, z_k)\,, & (i,k) \in [2, \mathrm{N_x}-1] \times [1, \mathrm{N_z}-1]\,. \end{cases} \tag{12b}$$

$$(\bar{F}_h)_i = \begin{cases} 0\,, & i \in \{1, \mathrm{N_x}\}\,, \\ \left(\Pi_h(F_h)\right)_i\,, & i \in [2, \mathrm{N_x}-1]\,; \end{cases} \tag{12c}$$

The solution $(\bar{\Phi}_h, \Phi'_h)$ *of the linear system* (12) *verifies*

$$(\partial_z^h \Phi'_h)_{i,\mathrm{N_z}-1/2} = 0, \quad i \in [2, \mathrm{N_x}-1]. \tag{13}$$

The Singular Perturbation problem (2) *is discretized thanks to*

$$\left(\varepsilon\mathbb{A}_{\perp} + \mathbb{A}_{\parallel}\right)\Phi_h = \varepsilon F_h\,. \tag{14}$$

Proof. The consistency follows from the definition of the discrete operators. To establish the property (13), the equation providing Φ'_h is operated to write

$$\mathbb{A}_\parallel^\alpha \Phi'_h = \varepsilon \left(F_h - \mathcal{A}_\perp \bar{\Phi}_h - \mathbb{A}_\perp \Phi'_h \right) .$$

Summing the lines of this equation over $k = 2, \ldots, \mathrm{N_z} - 1$ for any $i \in [2, \mathrm{N_x} - 1]$ yields, owing to the conservative discretization of $\mathbb{A}_\parallel^\alpha$

$$(A_\parallel)_{i,\mathrm{N_z}-1/2} (\partial_z^h \Phi'_h)_{i,\mathrm{N_z}-1/2} - (A_\parallel)_{i,3/2} (\partial_z^h \Phi'_h)_{i,3/2} = L_z \left(\bar{\mathcal{A}}_\perp \bar{\Phi}_h + \bar{\mathbb{A}}_\perp \Phi'_h - \bar{F}_h \right)_i .$$

The right hand side of this equation is the i-th line of the linear system providing $\bar{\Phi}_h$ in (12a) and therefore vanishes. □

We can now state that the AP discretizations give rise to linear systems with a condition number uniformly bounded with respect to ε while the matrix of the standard discretization has a condition number which grows linearly with ε^{-1}.

Proposition 2.4. *Assuming $A_\perp = A_\parallel = 1$ the matrices $\left(\varepsilon \mathbb{A}_\perp + \mathbb{A}_\parallel^\alpha \right)$ have a condition number uniformly bounded with respect to ε,*

$$\mathrm{Cond}_2 \left(\mathbb{A}_\perp + \mathbb{A}_\parallel^\alpha \right) = \frac{\max\limits_i(\lambda_i) + \dfrac{1}{\varepsilon} \max\limits_k(\ell_k^\alpha)}{\min\limits_i(\lambda_i) + \dfrac{1}{\varepsilon} \min\limits_k(\ell_k^\alpha)} . \tag{15a}$$

The condition number of the matrix $\left(\varepsilon \mathbb{A}_\perp + \mathbb{A}_\parallel \right)$ is an increasing linear function of ε^{-1} with

$$\mathrm{Cond}_2 \left(\varepsilon \mathbb{A}_\perp + \mathbb{A}_\parallel \right) = \frac{\max\limits_i(\lambda_i) + \dfrac{1}{\varepsilon} \max\limits_k(\ell_k)}{\min\limits_i(\lambda_i)} , \tag{15b}$$

with

$$\begin{aligned}
\lambda_i &= \frac{4}{(\Delta x)^2} \sin^2 \left(\frac{\pi k}{2(\mathrm{N_x} - 2)} \right) , \quad i = 1, \ldots, \mathrm{N_x} - 2 \\
\ell_k &= \frac{4}{(\Delta z)^2} \sin^2 \left(\frac{\pi \, (k-1)}{\mathrm{N_z} - 2} \right) , \quad \ell_k^D = \frac{4}{(\Delta z)^2} \sin^2 \left(\frac{\pi \, (k - 1/2)}{2(\mathrm{N_z} - 1)} \right) , \quad k = 1, \ldots, \mathrm{N_z} - 2 , \\
\ell_k^M &= \frac{4}{(\Delta z)^2} \sin^2 \left(\frac{\pi \, k}{2(\mathrm{N_z} - 2)} \right) , \quad k = 1, \ldots, \mathrm{N_z} - 3 , \qquad \ell_{\mathrm{N_z}-2}^M = \frac{1}{\Delta z^2} .
\end{aligned} \tag{15c}$$

The proof of this proposition is deferred to appendix A.

2.4 Strategy for an efficient Asymptotic-Preserving iterative resolution

2.4.1 Iterative resolution process

The main advantage of the AP formulations introduced in this paper is to avoid a Saddle point problem. Incorporating the zero mean constraint in the system matrix brings to main advantages. This is beneficial for the efficiency of the method, since it reduces the size of matrix, the unknowns associated to the Lagrangian being dropped. However, the gain remains marginal. Indeed the size of the Lagragian block counts $\mathrm{N_x}$ lines when the one associated to solution component is $\mathrm{N_x} \cdot \mathrm{N_z}$. The second advantage of these formulations is related to the property of the matrix $\varepsilon\mathbb{A}_\perp + \mathbb{A}_\parallel^\alpha$ which is invertible for $\varepsilon \geq 0$. Moreover the numerical methods used for standard elliptic problem should be efficient for the resolution of this problem. This is a property we wish to exploit in order to improve the efficiency of the AP method. The two components of the solution are thus iteratively updated , until convergence, thanks to the *external iterations*

$$\bar{\mathcal{A}}_\perp \bar{\Phi}_h^{(k+1)} = \bar{F}_h - \overline{\mathbb{A}}_\perp (\Phi'_h)^{(k)}, \tag{16a}$$

$$\left(\varepsilon\mathbb{A}_\perp + \mathbb{A}_\parallel^\alpha\right) (\Phi'_h)^{(k+1)} = \varepsilon F_h - \varepsilon\mathcal{A}_\perp \bar{\Phi}_h^{(k+1)}. \tag{16b}$$

A similar iterative resolution was considered in the first developments of the method [18, 8] however, with the Saddle point problem formulation solved by sparse direct solvers. The systems providing both components of the solution in the new formulations have the properties common to regular elliptic problems for which preconditioners can easily be constructed. Other numerical methods classically efficient for elliptic problems, for instance multigrid methods, should provide efficient resolution. We also aim to take advantage of one important property of the solution decomposition. One of the component only depends on the perpendicular coordinates. Therefore, the computational cost of this part of the solution is negligible compared to that of the three dimensional part. The strategy developed here, consists therefore in performing few *internal iterations*, in order to update the three dimensional component with a poor precision, then to compute a precise iterate of the less resource demanding two dimensional one. The purpose of such a procedure is to offset the overhead characteristic of AP formulations, which requires the resolution of the system for two unknowns. By this mean, we wish to reduce the computational requirements of the AP method to that of the system providing the component with non vanishing aligned gradient, which should be close to the computational effort required to solve a standard elliptic problem.

Remark 2.2. *Note that the iterative resolution* (16) *does not carry out iterates compliant with the boundary conditions along the z-coordinate, i.e. with* $(\partial_z^h \phi'^k)_{i,\mathrm{N_z}} = 0$. *Indeed, summing the lines of the discrete fluctuation equation (16b) yields*

$$\begin{aligned}\frac{(A_\parallel)_{i,\mathrm{N_z}-1/2}}{L_z}\left(\partial_z^h \Phi'_h\right)_{i,\mathrm{N_z}-1/2} - \frac{(A_\parallel)_{i,3/2}}{L_z}\left(\partial_z^h \Phi'_h\right)_{i,3/2} &= -\varepsilon\left(\bar{\mathcal{A}}_\perp \bar{\Phi}_h^{(k+1)} + \bar{\mathbb{A}}_\perp \Phi_h^{\prime(k+1)} - \bar{F}_h\right)_i \\ &= -\varepsilon\bar{\mathbb{A}}_\perp(\Phi_h^{\prime(k+1)} - \Phi_h^{\prime(k)})_i.\end{aligned}$$

However, the right hand side of this equation vanishnig at convergence, the consistency with the set of boundary conditions is thus recovered.

2.4.2 Control of the internal iterations

In the sequel the internal iterations refer to the update of $(\Phi'_h)^{(k+1)}$ thanks to $\bar{\Phi}_h^{(k+1)}$ by solving (16b). The convergence of the iterative method implemented to this end (a preconditionned Krylov method) is classically controlled by means of a backward error analysis which is reworked in order to enslave the convergence of the internal iterations with that of the external iterations alternating (16a) and (16b)).

Two controls are defined for the resolution of the problem (16b)

$$\tau_R^{(k+1,\mathcal{I})} := \|\varepsilon\mathcal{A}_\perp\bar{\Phi}_h^{(k+1)} - \varepsilon F_h\|_1 / \|r^{(k+1,\mathcal{I}))}\|_1\,, \tag{17a}$$

$$\begin{aligned}\tau_A^{(k+1,\mathcal{I})} &:= \|r^{(k+1,0}\|_1 / \|r^{(k+1,\mathcal{I}))}\|_1\,,\\ r^{(k+1,\mathcal{I})} &:= \left(\varepsilon\mathbb{A}_\perp + \mathbb{A}_\parallel^M\right)(\Phi'_h)^{(k,\mathcal{I})} + \varepsilon\mathcal{A}_\perp\bar{\Phi}_h^{(k+1)} - \varepsilon F_h\,;\end{aligned} \tag{17b}$$

where k and $\mathcal{I}$ denote respectively the current external and internal iteration count. The new iterate $(\Phi'_h)^{(k+1)} := (\Phi'_h)^{(k+1,\mathcal{I})}$ is obtained for an internal iteration count $\mathcal{I}$ verifying one of these two conditions

$$\tau_R^{(k+1,\mathcal{I})} < \mathcal{E}_R\,, \tag{18a}$$

$$\tau_A^{(k+1,\mathcal{I})} < \alpha\,, \tag{18b}$$

where $\mathcal{E}_R$ and α are parameters defining the precision required for the iterative solver.

The criterion $\tau_R^{(k+1,\mathcal{I})}$ controls the precision of the computations relative to the norm of the right hand side of the system (16b). It is classically referred to as the relative residual control. The parameter $\tau_A^{(k+1,\mathcal{I})}$ evaluates the initial residual associated to the computation of $(\Phi'_h)^{(k+1)}$, $\alpha < 1$ being the decreasing factor which defines a convergence criterion more and more stringent with the increase of the external iteration count. This is related to the absolute residual norm tolerance classically implemented to monitor iterative solvers based on Krylov subspace methods [31, 32].

During the first external iterations $k \sim 1$, $\|r^{(k+1,0)}\|_1$ is large, therefore a coarse precision is required for the internal iterations. Note that a tight convergence of the internal iterations would be ineffective since the initial estimates of $\bar{\Phi}_h$ are not precise either. Conversely, for large values of k the precision imposed to the internal iterations is more demanding since the $\|r^{(k+1,0)}\|_1 \to 0$ with $k \to +\infty$. By this means, the convergence of the more demanding iterative solver, the one carrying out the iterates of the three dimensional component Φ_h, is more and more severe with the precision of $\bar{\Phi}_h^{(k+1)}$ improved with the external iterations.

2.4.3 Control of the external iterations

Two types of criteria are combined to control the external iterations. The first one is the number of internal iterations $\mathcal{I}$ required to achieve convergence. The convergence of the

external iterations are assumed when the convergence of the internal ones is stopped by the criterion (18a). This is diagnosed by $\mathcal{I} = 1$ since the value of α is small enough to assume that the residual norm can not be decreased by a factor α in a single iteration. This means that the computation of the three dimensional component has reached the required precision and that the other component will not be improved either.

The second criterion relies on the difference of two consecutive iterates *i.e.* with

$$\tau_S := \|(\Phi'_h)^{(k+1)} - (\Phi'_h)^{(k)}\|_2 / \|(\Phi'_h)^{(k+1)}\|_2 \,, \tag{19}$$

the convergence of the external iterations being assumed when this criterion is below a given threshold $\tau_S < \mathcal{E}_S$. The algorithm of iterative resolution is described in Algorithm 1.

Algorithm 1 Iterative resolution of the AP Schemes: controls of the internal and external iterations.

1: Initialize the convergence tolerances $\mathcal{E}_R \ll 1$, $\mathcal{E}_S \ll 1$ and $\alpha < 1$.
2: Initialize $(\Phi'_h)^{(0)}$ and solve for $(\bar{\Phi}_h)^{(1)}$ and $(\Phi'_h)^{(1)}$.
3: Initialize the internal iteration count $\mathcal{I} = \infty$.
4: Initialize the External Iteration count k = 1.
5: **while** ($\mathcal{I} > 1$ and $\tau_S > \mathcal{E}_S$) **do**
6: Compute $(\bar{\Phi}_h)^{(k+1)}$ by solving the equation (16a).
7: Improve $(\Phi'_h)^{(k+1,\mathcal{I})}$ thanks to Eq. (16b) until $\tau_A^{(k+1,\mathcal{I})} < \alpha$ or $\tau_R^{(k+1,\mathcal{I})} < \mathcal{E}_R$.
8: Set $(\Phi'_h)^{(k+1)} := (\Phi'_h)^{(k+1,\mathcal{I})}$.
9: Update the actual value $\mathcal{I}$ from the internal iteration solver.
10: Set $k = k + 1$.
11: **end while**

3 Numerical investigations

3.1 Setup definition

A manufactured solution is carried out in order to validate the numerical methods by comparison with analytic estimates. For two dimensional problems the following solution will be used

$$\phi(x, y, z) = \sin\left(\frac{4\pi x}{L_x}\right) \sin\left(\frac{4\pi y}{L_y}\right) \left(1 + \varepsilon \cos\left(\frac{2\pi z}{L_z}\right)\right), \tag{20a}$$

with the diffusion coefficients defined by

$$A_x(x, y, z) = 1 + xz^2, \qquad A_y(x, y, z) = (1 + yz^2)\,, \qquad A_\parallel(x, y, z) = 1 + xz. \tag{20b}$$

The two dimensional setup is derived from (20) by setting $y = L_y/8$ and $A_\perp = A_x$. The function f is analytically computed to define the right hand side of the problem. Heterogeneous anisotropies will also be investigated with an asymptotic parameter undergoing

large variations in the computational domain. To this end the following definition will be considered

$$\varepsilon(z) = \frac{1}{2}\left(\varepsilon_{\max}(1+\tanh(R(L_z/2-z))) + \varepsilon_{\min}(1-\tanh(R(L_z/2-z)))\right), \quad R = 35\,. \quad (21)$$

The bounds $\varepsilon_{\min}$ and $\varepsilon_{\max}$ are test case specific and will be detailed in the next lines.

3.2 Conditioning of the system matrix

In this section we analyze the condition number of the system matrices issued from the discretization of the different formulations. These investigations are focused on the system providing the component of the solution with non vanishing parallel gradient. The aim is to provide a numerical estimation of the condition number evolution with respect to either the mesh size or the asymptotic parameter. This analysis is carried out for a two dimensional framework with homogeneous asymptotic parameter and diffusion coefficients ($A_\perp = A_\parallel = 1$) which is compliant with the estimations of Prop. 2.4.

The computed estimates of the matrices condition number are compared to the analytic estimates provided by Prop. 2.4 on Fig. 1. A linear growth is observed for the matrix defined by Eq. (14) stemming from the discretization of the singular problem. The condition numbers of the AP schemes remain almost uniform. The values computed are in a good agreement with the analytic estimates.

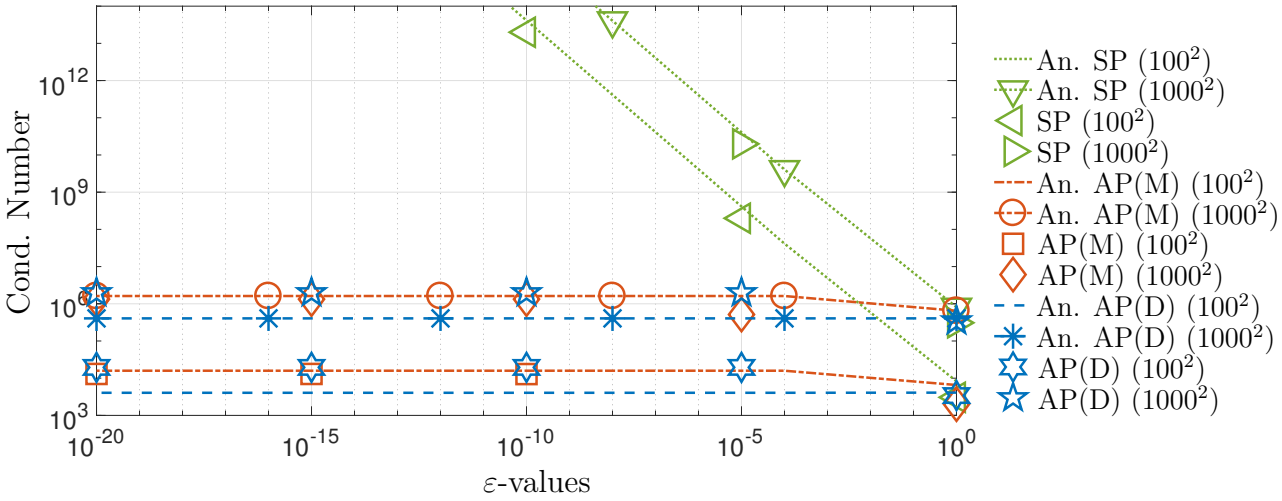

Figure 1: Condition number estimates for the discretization matrices of the Singular Perturbation problem $\left(\varepsilon\mathbb{A}_\perp + \mathbb{A}_\parallel\right)$ and the AP schemes $\left(\varepsilon\mathbb{A}_\perp + \mathbb{A}_\parallel^\alpha\right)$ denoted AP(M) and AP(D), computed by the MUMPS solver [1, 2]) as functions of the anisotropy ratio. The analytic estimates (An.) derived in Prop. 2.4 are plotted against the approximation computed from the system matrices for meshes with 100×100 and 1000×1000 cells.

3.3 Convergence of the method

The investigations performed in this section are devoted to demonstrate the numerical convergence of the method and that the formulations avoiding the Saddle point problem preserve the properties of AP-schemes. The computations are limited to two dimensional simulations in order to easily carry out numerical approximations on refined meshes. A solution is manufactured in order to quantify precisely the approximation error of the numerical method with either a uniform ε parameter or, an anisotropy ratio with spatial variations. In the sequel, we will consider the following solution

The aim here is to investigate the convergence of the new AP formulations with either a direct resolution of the system as stated by Eq. (12) or the iterative process (16). We emphasize that standard preconditioners are ineffective for the resolution of the global system (a similar conclusion was made in [8], this issue is also pointed out in [3]). Therefore the convergence of (non-preconditionned) iterative solvers is too slow to be considered as an alternative to sparse direct solvers. The convergence results are reported on Fig. 2. The two AP formulations providing equivalent convergence results, only one plot is displayed for both formulations. The MUMPS solver [1, 2] is used for direct resolution. The inner problems of the iterative resolution are solved by standard a Krylov method, namely a flexible GEMRES method with a Krylov subspace size equal to 10 (FGEMRES(10)) preconditionned thanks to an incomplete LU factorization with diagonal compensation (ILUD with dropping threshold set to 10^{-3}) [31, 32]. From Fig. 2 we observe that the convergence rate of the methods is unaffected by the anisotropy strength.

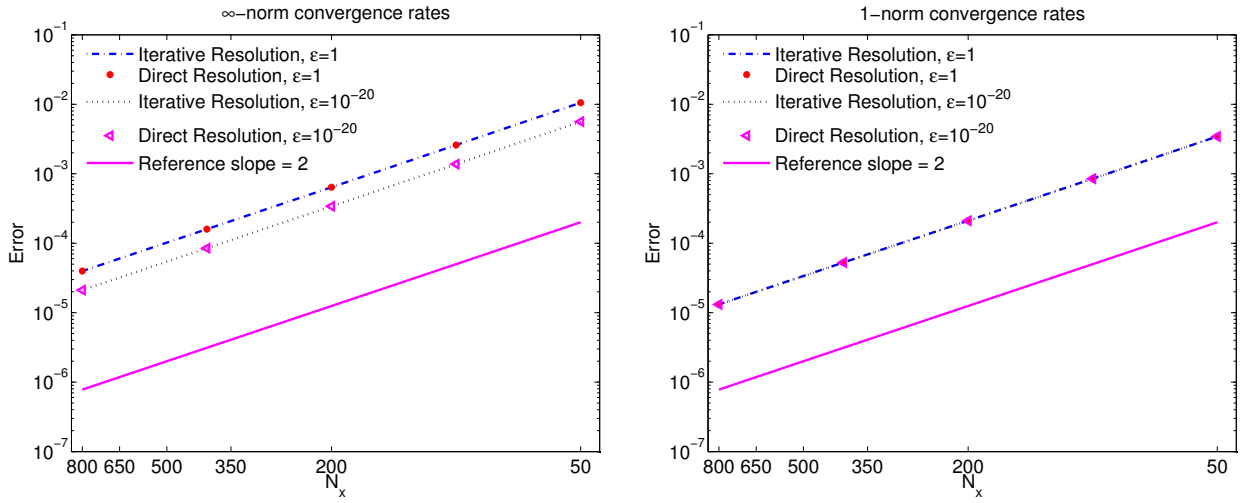

(a) Error ℓ_∞-norm.

(b) Error ℓ_1-norm.

Figure 2: The convergence rate for the AP schemes for homogeneous anisotropy ratios: Error norms between the numerical approximation and the analytic solution of the solution component with a non vanishing aligned gradient as functions of the mesh size.

The same investigations are performed for heterogeneous anisotropy ratios, with ε defined by Eq. (21) and $\varepsilon_{\min}$ ranging from 1 to 10^{-20} ε_{max} being set to 1. The results are plotted on Fig. 3 with similar conclusions to that of the homogeneous case.

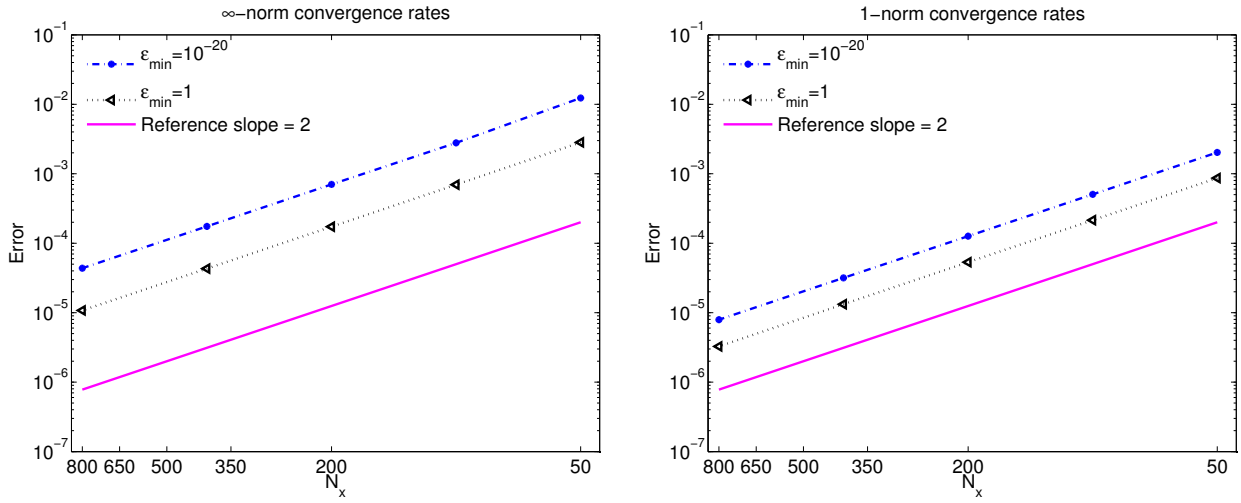

(a) Error ℓ_∞-norm.

(b) Error ℓ_1-norm.

Figure 3: Convergence rate for the AP schemes for heterogeneous anisotropy ratios: Error norms between the numerical approximation and the analytic solution of the solution component with a non vanishing aligned gradient as functions of the mesh size.

3.4 Efficiency improvements

In this section a comparison of the numerical efficiency of the different solvers is conducted. As a reference the direct sparse solver used so far is considered. The aim of this section is to highlight the tremendous gains in efficiency the methods introduced in this paper bring, compared to the precedent achievements. In particular, it should be pointed out that sparse direct solvers, while competitive in term of computational efforts for two dimensional problems, give a picture totally different for problem solved in a three dimensional space. Hence the motivation of the present work outlined in the next lines.

3.4.1 Lexicographic orderings

The importance of the unknowns ordering on the preconditionning efficiency is outlined in the literature [4]. For anisotropic diffusion, it is observed that an ordering along the direction with a weak diffusion is more efficient, which is somehow counter-intuitive [9]. We provide here a numerical investigation of different lexicographic orderings and analyze their influence on the iterative solver efficiency.

The ordering is identified in the precedent sections by the function I. Here we define I_1 a weak-first ordering, I_2 a weak-last ordering and I_3 a weak-second ordering :

$$\begin{aligned} I_1 &= i + (j-1) \times \mathrm{N_x} + (k-1) \times \mathrm{N_x} \times \mathrm{N_y}, \\ I_2 &= k + (j-1) \times \mathrm{N_z} + (i-1) \times \mathrm{N_y} \times \mathrm{N_z}, \\ I_3 &= j + (k-1) \times \mathrm{N_y} + (i-1) \times \mathrm{N_y} \times \mathrm{N_z}. \end{aligned} \tag{22}$$

Note that with the ordering defined by I_2 the unknowns along the anisotropy direction are contiguous. Conversely, with definition I_1 a change in the direction of the anisotropy (related to k) is translated by a large variation (proportional to $\mathrm{N_x} \times \mathrm{N_y}$) of the associated matrix rank.

The aim here is to analyze the effectiveness of the resolution of the three dimensional problems which represent barely the entire computational effort of the AP scheme resolution. The exact two dimensional component of the solution is injected into the three dimensional problem which is solved only once. The preconditionner is computed by a standard incomplete LU factorization implementing a dropping strategy and a diagonal compensation (ILUD with a default dropping parameter set to 10^{-3}) complementing a GEMRES method [31, 32]. The results relating the resolution of the three dimensional component of the AP formulations as well as the resolution of the orginal problem are reported in Table 1.

Regarding the resolution of the isotropic original (SP) problem, *i.e.* for $\varepsilon = 1$, none of the orderings can be picked out as a best guess regarding the overall computational time. With respect to the precondionner density the strong-last ordering I_1 is slightly more efficient than the strong-first orderings I_2 and I_3 that require more time to compute the preconditionner and more memory storage, in return for better convergence rates. For a weak anisotropy strength ($\varepsilon = 10^{-3}$), the strong-last ordering I_1 is observed to be the most efficient, the weak-last ordering I_2 being the most resource demanding which is consistent with the conclusion in [9]. However the efficiency improvement remains moderate, lower than 10% on the overall computational time.

For the AP schemes, the weak-last orderings I_2 and I_3 are more efficient than the strong-last ordering I_1. This is particularly striking for the isotropic framework and specifically for the AP(M) formulation. This differences trail off for anisotropic configurations the weak-last ordering I_2 remaining the most efficient out of the panel, however still with a small margin (at most 20%) regarding the computational time. In the sequel the weak-last orderings I_2 is used for all the computations.

Note that for most severe anisotropies ($\varepsilon > 10^{-4}$) the convergence of the iterations can hardly be achieved for the SP problem whatever the values of the parameter used to compute the preconditionner. Conversely, the performance of the iterative solver remains unaffected for both AP formulations. Another important feature should be pointed out regarding the effectiveness of the approach developed here. Note, indeed, that the resolution of an anisotropic problem is less time and memory consuming than that of the isotropic problem. The most efficient AP formulation proves to be the AP(M) formulation with a computational time barley divided by 10^2 compared to the resolution of an isotropic SP problem by iterative methods.

Table 1: Efficiency of the preconditioner with respect to the orderings defined by Eq. (22) on a $(100 \times 100 \times 100)$ mesh for the matrices $(\varepsilon \mathbb{A}_{\perp} + \mathbb{A}_{\parallel})$ and $(\varepsilon \mathbb{A}_{\perp} + \mathbb{A}_{\parallel}^{\alpha})$ issued respectively from the discretization of the Singular Perturbation problem (SP) and the AP(M) and AP(D) formulations: preconditioner non zeros elements count relative to that of the matrix, time of computation of the preconditioner, number of iterations to reach convergence, computational time for the resolution and total computational time (preconditioner and iterations).

(a) SP problem with $\varepsilon = 1$

Ordering	I_1	I_2	I_3
Density	10.68	12.43	13.04
Time Prec.	1.18e+1	1.63e+1	1.99e+1
Its	52	27	26
Time Sol.	1.16e+1	7.00	7.10
Total Time	2.34e+1	2.33e+1	2.70e+1

(b) SP problem with $\varepsilon = 10^{-3}$

I_1	I_2	I_3
0.48	0.47	0.47
1.04e-1	1.04e-1	1.04e-1
44	47	47
1.62	1.84	1.70
1.72	1.94	1.80

(c) AP(M) scheme with $\varepsilon = 1$

Ordering	I_1	I_2	I_3
Density	61.91	14.19	14.74
Time Prec.	4.74e+2	3.06e+1	4.59e+1
Its	47	51	44
Time Sol.	5.92e+1	1.66e+1	1.49e+1
Total Time	5.33e+2	4.72e+1	6.08e+1

(d) AP(M) scheme with $\varepsilon = 10^{-3}$

I_1	I_2	I_3
0.50	0.50	0.50
1.92e-1	1.44e-1	1.48e-1
3	3	3
1.48e-1	1.44e-1	1.36e-1
3.40e-1	2.88e-1	2.84e-1

(e) AP(D) scheme with $\varepsilon = 1$

Ordering	I_1	I_2	I_3
Density	12.85	13.31	12.86
Time Prec.	1.96e+2	2.06e+1	1.95e+1
Its	39	29	29
Time Sol.	1.11e+1	8.52	8.30
Total Time	3.07e+2	2.91e+1	2.78e+1

(f) AP(D) scheme with $\varepsilon = 10^{-3}$

I_1	I_2	I_3
0.57	0.55	0.57
1.08e-1	1.08e-1	1.08e-1
46	36	46
1.80	1.51	1.84
1.91	1.62	1.95

Finally the resolution of the entire anisotropic problem is investigated. Two alternatives are proposed, the first one consists in solving the matrix stemming from the discretization of the Singular-Perturbation problem thanks to a sparse direct solver. This approach is effective for moderate anisotropy ratios, however the precision of the numerical approximation can not be preserved with the matrix conditioning deterioration at large anisotropy strengths. This fact has already been pointed out in precedent works (see for instance [18]). The second approach relies on the iterative resolution of the AP discretizations. The computational time and the memory usage of both methods are presented on Fig. 4. The advantage of the iterative AP methods are all the more effective as the anisotropy is severe. In particular the bad scaling of the memory footprint and time consumption of the sparse direct solver for three dimensional problems appears clearly. The resolution of the problem requires 90, 230 and 400 times more storage for the factorized matrix compared to that of the discretized SP problem on meshes with 50^3, 100^3 and 150^3. To give some order of magnitudes, the factorized matrix consumes 0.3, 4 and 78 Go of memory for the mesh. For iterative AP resolutions, the memory footprint is significantly reduced for isotropic problems ($\varepsilon = 1$). Due to the discretization of the mean constraints the matrix of the AP(M) scheme consumes more memory than that of the SP model, however the preconditioner is less expensive than the sparse factorization with a 0.01, 0.1 and 0.4 Go memory footprint for the isotropic case and $7 \cdot 10^{-4}$, $7 \cdot 10^{-3}$ and $2.5 \cdot 10^{-2}$ Go for $\varepsilon = 10^{-3}$. This is 3 to 4 orders of magnitude less compared to the sparse solver in the most favorable configurations. The time consumption follows the same trend, with a gain for the largest mesh between 10 to 70 for the isotropic computations and 300 to $2 \cdot 10^4$ for $\varepsilon < 10^{-3}$. Note that none of the settings for either the direct sparse solver or the iterative methods are optimal, significant gains may still be expected thanks to specific tuning.

3.5 Demonstrative computations in the framework of ionospheric plasma simulation

The purpose of this section is to outline further the advantages of an iterative resolution of the system matrix for time evolving problems. Indeed, a good approximation of the solution can be provided by the solution of the preceding time step which may improve the efficiency of the method. With this aim, a real scale problem is investigated, in the frame of ionospheric plasma simulation thanks to the so-called Dynamo-3D model [5]. In its simplest form, this model couples a three dimensional transport equation evolving the plasma density n to a three dimensional anisotropic elliptic equation providing the electric potential ϕ, the velocity of the plasma u being deduced from the electric field thanks to a mobility relation.

Table 2: Iterative resolution of the AP(M) and AP(D) schemes for different mesh sizes and anisotropy ratios: external iterations and total iteration counts of the GEMRES method for the resolution of the three dimensional problem, total computational time (preconditioner construction and resolution of the coupled system) and error between the numerical approximation and the exact solution in ℓ_1-norm.

(a) $AP(M)$, $50 \times 50 \times 50$.

ε	α	10^{-1}	10^{-2}	10^{-3}	10^{-4}
1	Ex. It	6	4	4	4
	Tot. It	14	33	53	65
	Time	6.04e-1	1.48	2.12	2.63
	Error	3.22e-3	2.14e-3	2.14e-3	2.14e-3
10^{-2}	Ex. It	2	3	4	3
	Tot. It	3	7	18	28
	Time	7.60e-2	1.68e-1	4.24e-1	6.48e-1
	Error	2.19e-3	2.14e-3	2.14e-3	2.14e-3
10^{-4}	Ex. It	1	1	1	2
	Tot. It	1	1	1	4
	Time	1.20e-2	1.20e-2	1.20e-2	3.20e-2
	Error	2.14e-3	2.14e-3	2.14e-3	2.14e-3

(b) $AP(D)$, $50 \times 50 \times 50$.

ε	α	10^{-1}	10^{-2}	10^{-3}	10^{-4}
1	Ex. It	75	75	75	75
	Tot. It	300	450	600	750
	Time	9.94	1.5e+1	2.0e+1	2.5e+1
	Error	1.86e-3	1.84e-3	1.84e-3	1.84e-3
10^{-2}	Ex. It	14	10	10	10
	Tot. It	27	48	68	86
	Time	5.88e-1	9.70e-1	1.35	1.73
	Error	2.14e-3	2.13e-3	2.13e-3	2.13e-3
10^{-4}	Ex. It	1	1	4	4
	Tot. It	1	1	8	11
	Time	1.20e-2	1.20e-2	6.00e-2	7.20e-2
	Error	2.14e-3	2.14e-3	2.14e-4	2.14e-4

(c) $AP(M)$, $100 \times 100 \times 100$.

ε	α	10^{-1}	10^{-2}	10^{-3}	10^{-4}
1	Ex. It	3	6	4	4
	Tot. It	13	69	114	142
	Time	5.20	2.6e+1	4.1e+1	5.2e+1
	Error	6.92e-3	5.35e-4	5.29e-4	5.29e-4
10^{-2}	Ex. It	2	2	3	3
	Tot. It	5	9	23	43
	Time	1.14	2.00	4.97	9.14
	Error	7.15e-4	5.35e-4	5.34e-4	5.34e-4
10^{-4}	Ex. It	1	1	2	2
	Tot. It	1	1	4	4
	Time	9.2e-2	9.2e-2	2.68e-1	3.4e-1
	Error	5.34e-4	5.34e-4	5.34e-4	5.34e-4

(d) $AP(D)$, $100 \times 100 \times 100$.

ε	α	10^{-1}	10^{-2}	10^{-3}	10^{-4}
1	Ex. It	74	74	74	74
	Tot. It	444	738	1036	1300
	Time	1.4e+2	2.3e+2	3.2e+2	4.0e+2
	Error	7.07e-4	6.90e-4	6.90e-4	6.90e-4
10^{-2}	Ex. It	11	10	10	10
	Tot. It	51	81	124	168
	Time	1.1e+1	1.7e+1	2.5e+1	3.3e+1
	Error	5.32e-4	5.31e-4	5.31e-4	5.31e-4
10^{-4}	Ex. It	1	1	4	4
	Tot. It	1	1	11	15
	Time	8.80e-2	8.80e-2	5.68e-1	7.16e-1
	Error	5.35e-4	5.35e-4	5.34e-4	5.34e-4

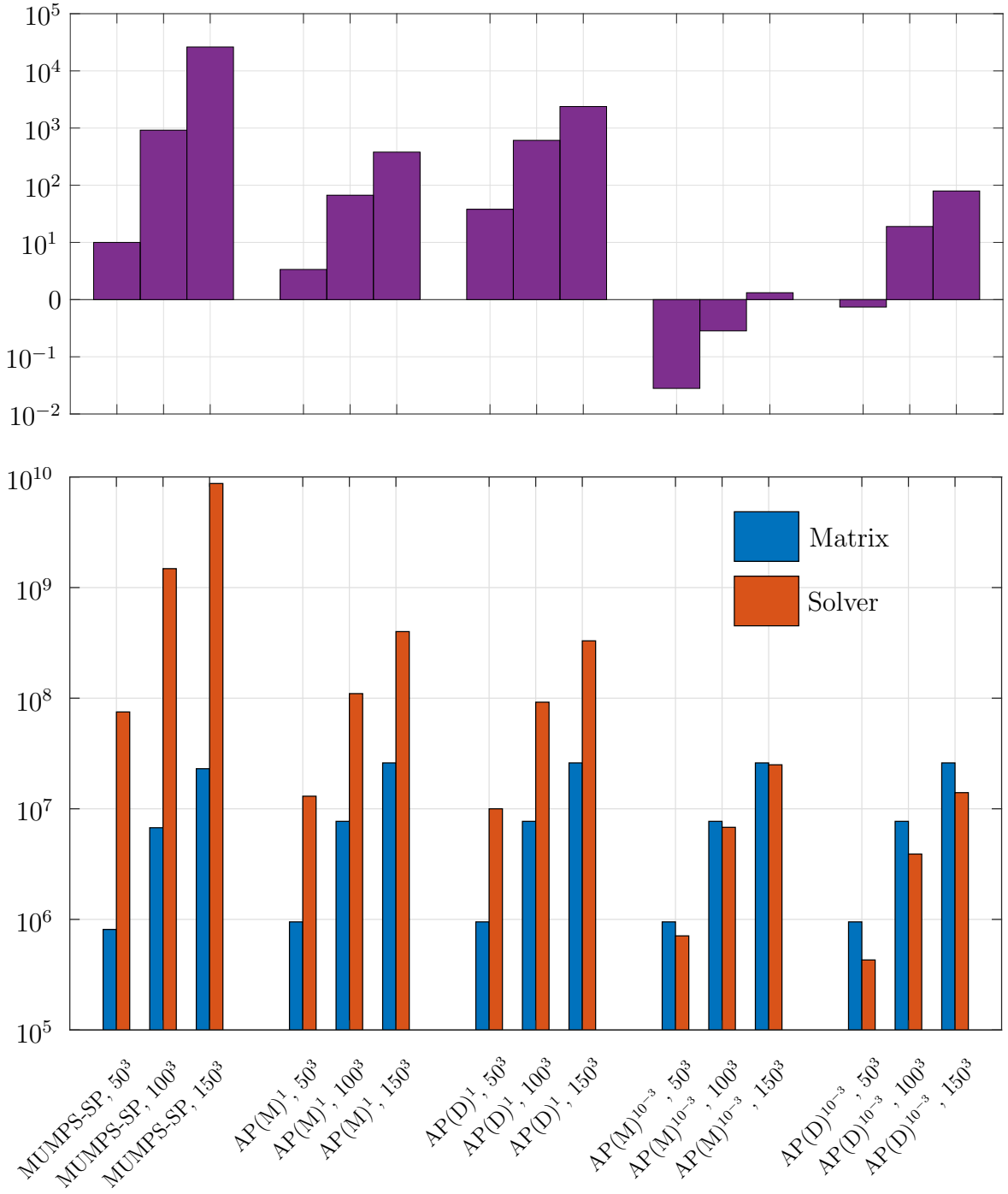

Figure 4: Cpu usage (top) and memory footprint (bottom) of a sparse direct solver for the Singular-Perturbation problem compared to the iterative resolution of the AP(M) and AP(D) schemes on meshes with 50^3, 100^3, and 150^3 cells: (top) computational time (Sec.) to solve the complete system (bottom) number of non zeros elements in the matrix of the Singular-Perturbation problem (MUMPS-SP), the AP(M) and the AP(D) formulations as well as the number of non zeros elements stored in the factorized matrix (MUMPS solver) and the preconditionner (AP methods). For the AP-schemes two setups are reported, one for $\varepsilon = 1$ the other for $\varepsilon = 10^{-3}$.

The simplified version of the model writes

$$\frac{\partial n}{\partial t} + \nabla \cdot (nu) = 0\,, \tag{23a}$$

$$-\nabla \cdot \Big(n\mathbb{M}\nabla\phi \Big) = -\nabla \cdot \Big(n\mathbb{M}_i \left(\kappa\varepsilon u_n\right) - n\mathbb{M}_e \left(\varepsilon u_n\right) \Big)\,, \tag{23b}$$

$$u = \mathbb{M}_i \left(E + \kappa\varepsilon u_n\right)\,, \tag{23c}$$

$$E = -\nabla\phi\,,$$

where the mobility matrices $\mathbb{M}_{\alpha,\,\alpha=e,i}$ and $\mathbb{M}$ are

$$\mathbb{M}_e = \begin{pmatrix} 0 & -1 & 0 \\ 1 & 0 & 0 \\ 0 & 0 & 1/\varepsilon \end{pmatrix}, \mathbb{M}_i = \begin{pmatrix} 0 & 1 & 0 \\ -1 & 0 & 0 \\ 0 & 0 & 1/\kappa\varepsilon \end{pmatrix}, \mathbb{M} = \begin{pmatrix} \kappa\varepsilon & 0 & 0 \\ 0 & \kappa\varepsilon & 0 \\ 0 & 0 & 1/\varepsilon \end{pmatrix}. \tag{23d}$$

In these equations the velocity of the neutral particles is denoted u_n, $\kappa = 10^2$ being the ratio of particle mobility between eletron and ion. The anisotropy variable is denoted by ε, which is much strong in high altitude of ionosphere ($\varepsilon \ll 1$) and becomes weak in low altitude ionosphere. Furthermore, all physical quantities in equations (23) are normalized in following simulation.

Introducing the operator $\nabla_\perp$ denoting the derivatives with respect to the transverse coordinates x and y, the equation providing the electric potential is recast into

$$-\nabla_\perp \cdot (n\kappa\varepsilon\nabla_\perp\phi) - \frac{\partial}{\partial z}\left(\frac{n}{\varepsilon}\frac{\partial\phi}{\partial z}\right) = f, \tag{24}$$

with the source term f defined as

$$f = -\frac{\partial}{\partial x}(nu_{n,y}) + \frac{\partial}{\partial y}(nu_{n,x}).$$

This simplified model is implemented in a computational domain Ω which consists of a magnetic field tube. For these computations the curvature of the magnetic field lines are also disregarded, the magnetic field being assumed aligned to the z-direction. The computational domain is decomposed into $\Omega_x \times \Omega_y \times \Omega_z = [-L_x, L_x] \times [-L_y, L_y] \times [0, L_z]$.

As a test case the development of the so-called Striation instability [6, 7] is reproduced for the first time thanks to a model that carry out a three dimensional electric potential. A uniform plasma density background ($n = 1$) is perturbed by an initial plasma bubble ($n = 2$) submitted to a neutral wind $u_n = (1, 0, 0)^T$, which initiates the developments of the instability on the side of the bubble unexposed to the neutral wind, as depicted on Fig. 5. Two frameworks are considered, defined by

CASE I: Uniform strong anisotropy, $\varepsilon = 10^{-5}$ which prevails at the highest altitudes. In this case the Dynamo model can be regarded as its asymptotic limit, the Striation model [5], derived under the assumption of infinite parallel mobilities.

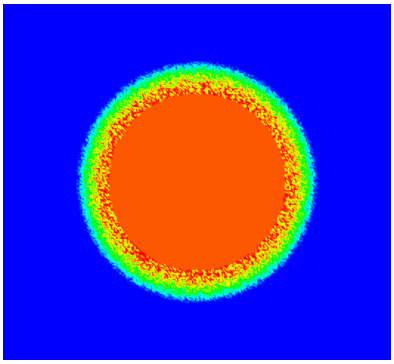

Case I: $t = 0$.

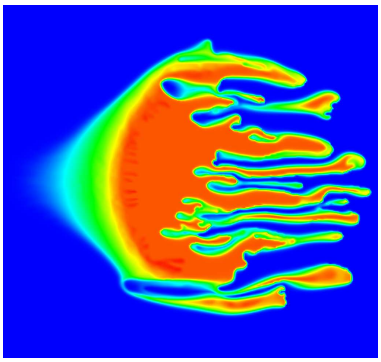

Case I: $t = 2.4$.

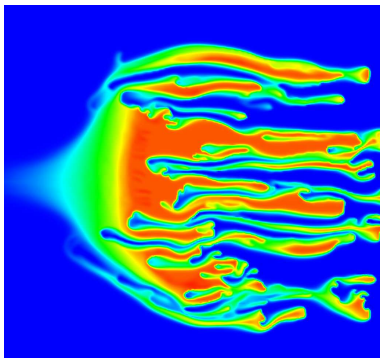

Case I: $t = 3.4$.

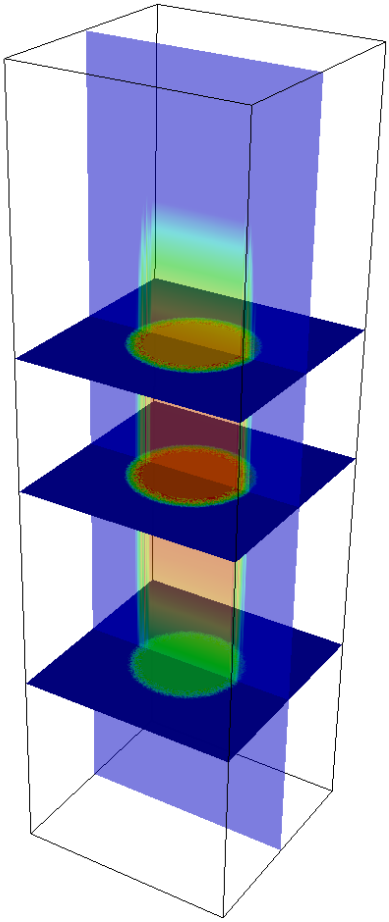

CASE II: $t = 0$.

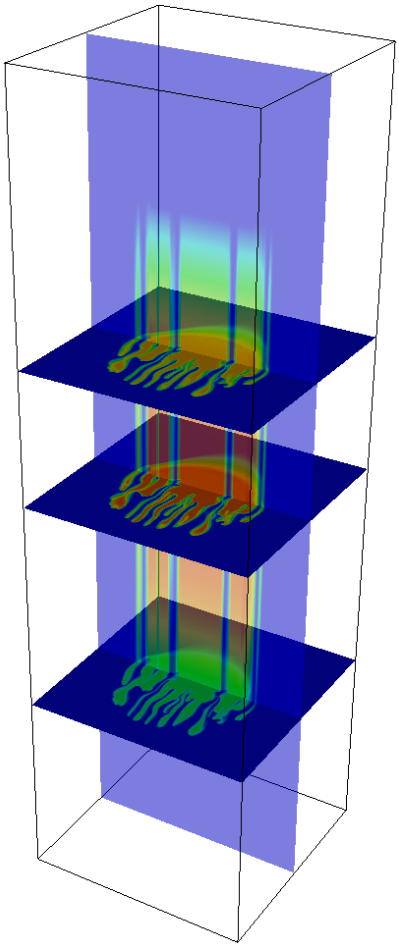

CASE II: $t = 6.4$.

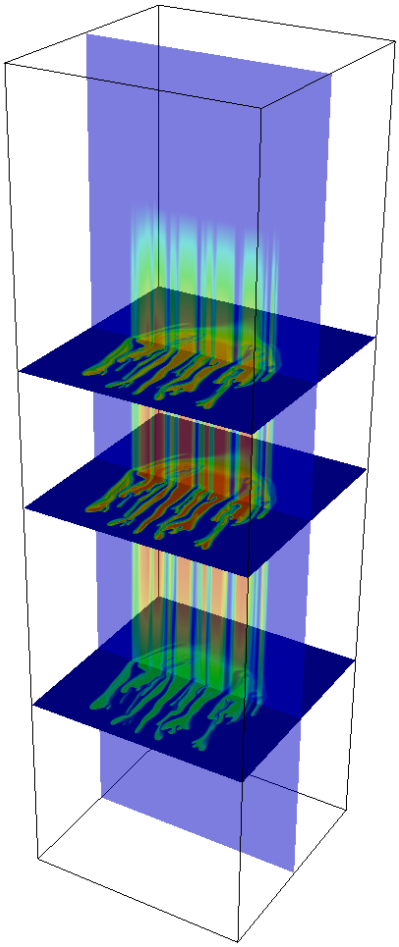

CASE II: $t = 10$.

Figure 5: Striation simulation with the parameters defined by Case I (homogeneous anisotropy) and Case II (heterogeneous ansitropy) carried on a mesh with $(\mathrm{N_x}, \mathrm{N_y}, \mathrm{N_z}) = (300, 300, 300)$. Top: plasma density as a function of the space variables in a plane orthogonal to the magnetic field; Bottom: plasma density in the three dimensional magnetic flux tube.

CASE II: Variable anisotropy, $\varepsilon \in [10^{-1}, 10^{-5}]$ which relates a larger range of altitudes, the anisotropy being weaker at the lowest altitudes where the limit model is not valid.

The elliptic equation (23b) is discretized by the AP(M) scheme described in Sec. 2.3. For the continuity equation (23a), we use the anti-dissipative advection scheme introduced in [35]. Finally, the advection velocities, depending on the potential, are computed thanks to standard second order finite difference methods.

The time evolution of the plasma density carried out on a mesh with 300^3 (27 millions) cells is reported on Fig. 5. The computations are in a good agreement with that of [7] computed with the Striation model in which the anisotropic elliptic equation is substituted by the limit problem verified by $\bar{\phi}$. However, this asymptotic limit of the Dynamo model is not valid for intermediate anisotropy ratios as the ones considered in the CASE II.

The purpose here is also to outline the gains that are possible regarding the efficiency of the computations taking advantage of the resolution of a time dependent problem. Indeed, the solution ϕ at time t^m defines a good guess to initiate the iterations providing the solution at time t^{m+1}. Furthermore, the same preconditionner can be carried out over multiple time steps before being updated. This is experienced in this framework as reported on Fig. 6 and 7. Substantial savings are obtained in the computational time required to carry out the solution. The number of internal iteration for the computation of the fluctuation (three dimensional component) is roughly divided by two. Note that the number of iterations required for the computation of $\bar{\phi}$ is also significantly reduced. The gains that follow a less frequent preconditionner update is quite marginal with a decrease of the computational time at best equal to 10%. The computational time required for the preconditionner update is partially offset by an altered rate of convergence.

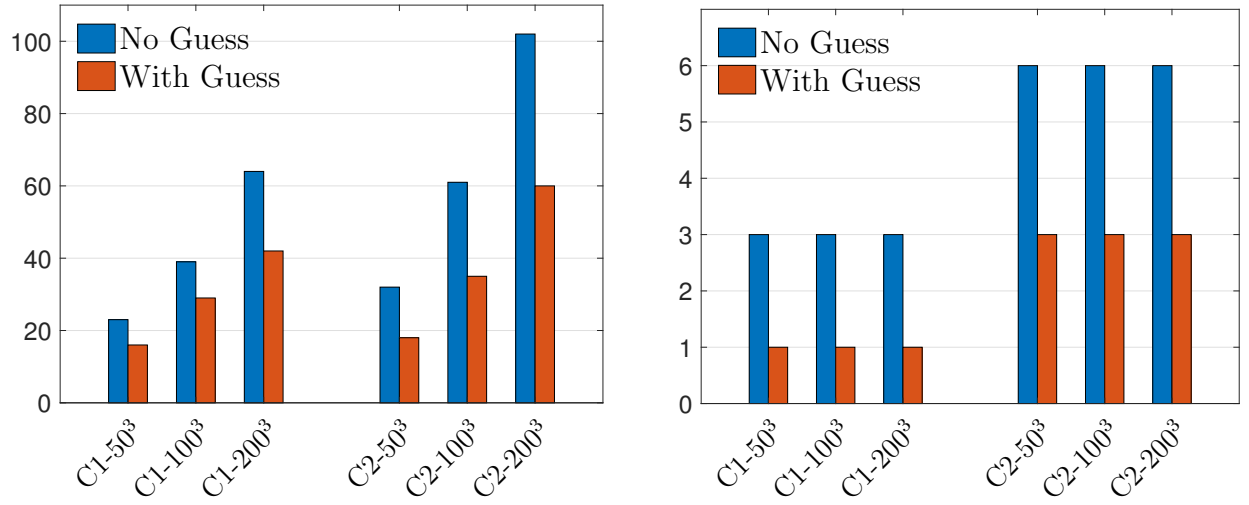

(a) Computation of $\bar{\phi}$.

(b) Computation of ϕ'.

Figure 6: Comparison of total iteration counts for the resolution of solution two components fore the CASE I (CI) and CASE II configurations (CII) with (or without) the solution at the precedent time step to initiate the iterative solver on mesh with 50^3, 100^3 and 200^3 cells.

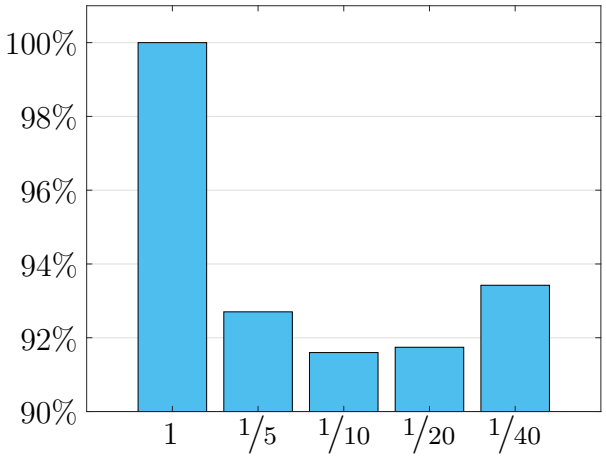

Figure 7: Computational time as a function of the preconditionner update frequency for simulations carried out on a 100^3 mesh with the setup CASE II. The reference (100%) is the simulation computational time for a preconditionner update each time step.

4 Conclusions

This paper is devoted to the development of Asymptotic-Preserving methods for the efficient three dimensional resolution of anisotropic elliptic problems. Precedent AP methods rely on a reformulation of the equation into a Saddle point problem for which only sparse direct solvers have been successfully operated and are limited to finite element discretizations. The development of these AP methods to the finite difference framework is addressed in the present paper. Two new Asympotic-Preserving formulations are also introduced with the advantage to be free from the resolution of a Saddle point problem. In contrast to standard methods, the condition number of the system matrices derived form these AP methods are demonstrated to be uniformly bounded with respect to the anisotropy ratio. To this end, we operate a decomposition of the solution into a component independent of the coordinate aligned with magnetic field complemented with a three dimensional component. These two functions verify elliptic problems for which classical solver can be efficiently implemented. The resolution of the coupled system proposed here consists thus of a fixed point iteration between the two components. We propose an enslavement of the internal iterations carried out for the three dimensional component computation with that of the outer iterations in order to preserve a computation cost of the AP methods comparable to that of the resolution of an isotropic problem. These developments bring significant gains in comparisons to precedent achievements with respect to memory and time consumption that are reduced by many orders of magnitude. This makes possible to address more physically relevant models on the required time and space scales addressed in a future work.

Acknowledgments

This work has been carried out within the framework of the EUROfusion Consortium and has received funding from the Euratom research and training programme 2014-2018 under grant agreement No 633053. The views and opinions expressed herein do not necessarily reflect those of the European Commission.
Furthermore, FD would like to acknowledge support from the ANR MOONRISE (MOdels, Oscillations and NumeRIcal SchEmes, 2015-2019).
This work has been initiated during the Post-Doc of JC supported by the ANR IODISSEE (IOnospheric DIsturbanceS and SatEllite-to-Earth communications, 2009-2014).

A Estimations of the matrix condition numbers

An estimation of the condition number for different matrices stemming from the discretization of the AP reformulations as well as the singular perturbation problem is provided in this section. To this end, the diffusion coefficients are assumed to be equal to one, the purpose being to outline the property of the different methods with respect to the asymptotic parameter. In this simplified framework, the linear system associated with the discretization of the singular perturbation problem (2) is recast into

$$\frac{1}{(\Delta x)^2}\mathbb{M}_N^{dd}\Phi_h + \frac{1}{\varepsilon}\frac{1}{(\Delta z)^2}\Phi_h\mathbb{M}_N^{nn} = F_h\,,$$

with $\Phi_h = (\phi_{i,k})_{i,k=1,\dots,N}$, $F_h = (f_{i,k})_{i,k=1,\dots,N}$, $\mathbb{M}_d$ and $\mathbb{M}_N$ four matrices of $\mathbb{R}^{N\times N}$ where

$$\mathbb{M}_N^{dd} := \begin{pmatrix} 2 & -1 & 0 & \dots & 0 \\ -1 & 2 & -1 & \ddots & \vdots \\ 0 & \ddots & \ddots & \ddots & 0 \\ \vdots & \ddots & -1 & 2 & -1 \\ 0 & \dots & 0 & -1 & 2 \end{pmatrix}, \quad \mathbb{M}_N^{nn} := \begin{pmatrix} 1 & -1 & 0 & \dots & 0 \\ -1 & 2 & -1 & \ddots & \vdots \\ 0 & \ddots & \ddots & \ddots & 0 \\ \vdots & \ddots & -1 & 2 & -1 \\ 0 & \dots & 0 & -1 & 1 \end{pmatrix}.$$

The eigenvalues of the system matrix discretizing the problem (2) are denoted $\Lambda_{i,k}\,,\ (i,k) = 1,\dots,N$, they can be expressed thanks to $(\lambda_i)_{i=1,\dots,N}$ and $(\ell_k^{nn})_{k=1,\dots,N}$ the eigenvalues of respectively the matrices $\mathbb{M}_N^{dd}$ and $\mathbb{M}_N^{nn}$, with

$$\Lambda_{i,k} = \frac{1}{(\Delta x)^2}\lambda_i + \frac{1}{\varepsilon}\frac{1}{(\Delta z)^2}\ell_k^{nn}\,, \qquad (i,k) = 1,\dots,N\,. \tag{25}$$

Similarly the AP system providing the component of the solution with non vanishing aligned gradients can be stated as

$$\frac{1}{(\Delta x)^2}\mathbb{M}_N^{dd}\Phi_h + \frac{1}{\varepsilon}\frac{1}{(\Delta z)^2}\Phi_h\mathbb{M}_N^{nm} = \mathcal{F}_h\,, \tag{26a}$$

$$\frac{1}{(\Delta x)^2}\mathbb{M}_N^{dd}\Phi_h + \frac{1}{\varepsilon}\frac{1}{(\Delta z)^2}\Phi_h\mathbb{M}_N^{nd} = \mathcal{G}_h\,, \tag{26b}$$

the matrices $\mathbb{M}_N^{nm}$ and $\mathbb{M}_N^{nd}$ being defined and analyzed thanks to the following lemma.

Lemma A.1. *Let $\mathbb{M}_N^{nd}$ and $\mathbb{M}_N^{nm}$ be the matrices defined by*

$$\mathbb{M}_N^{nd} := \begin{pmatrix} 1 & -1 & 0 & \dots & \dots & 0 \\ -1 & 2 & -1 & \ddots & & \vdots \\ 0 & \ddots & \ddots & \ddots & \ddots & \vdots \\ \vdots & \ddots & -1 & 2 & -1 & 0 \\ 0 & \dots & 0 & -1 & 3 & 0 \\ 0 & \dots & 0 & 0 & 1 & 1 \end{pmatrix}, \quad \mathbb{M}_N^{nm} := \begin{pmatrix} 1 & -1 & 0 & \dots & 0 \\ -1 & 2 & -1 & \ddots & \vdots \\ 0 & \ddots & \ddots & \ddots & 0 \\ \vdots & \ddots & -1 & 2 & -1 \\ 1 & \dots & 1 & 0 & 2 \end{pmatrix}, \tag{27a}$$

the eigenvalues of these matrices are

$$\ell_k^{nd} = \begin{cases} 4\sin^2\left(\dfrac{\pi(k-1/2)}{2(N-1)}\right), & k = 1, \dots, N-1, \\ 1 & k = 1, \end{cases} \tag{27b}$$

$$\ell_k^{nm} = \begin{cases} 4\sin^2\left(\dfrac{\pi\, k}{2N}\right), & k = 1, \dots, N-1, \\ 1 & k = 1. \end{cases} \tag{27c}$$

The eigenvalues $(\lambda_i)_{i=1,N}$ and $(\ell_k^{nn})_{k=1,N}$ of the matrices $\mathbb{M}_N^{dd}$ and $\mathbb{M}_N^{nn}$ are defined by

$$\lambda_i = 4\sin^2\left(\frac{\pi i}{2(N+1)}\right), \qquad i = 1, \dots, N, \tag{27d}$$

$$\ell_k^{nn} = 4\sin^2\left(\frac{\pi(k-1)}{2N}\right), \qquad k = 1, \dots, N. \tag{27e}$$

Proof. We prove that the matrix $B := \mathbb{M}_N^{dm}$ has the same eigenvalues as the matrix $A \in \mathbb{R}^{N\times N}$, where

$$A := \begin{pmatrix} 2 & -1 & 0 & \dots & 0 & 0 \\ -1 & 2 & -1 & \ddots & \vdots & \vdots \\ 0 & \ddots & \ddots & \ddots & 0 & 0 \\ \vdots & \ddots & -1 & 2 & -1 & 0 \\ 0 & \dots & 0 & -1 & 2 & 0 \\ 0 & \dots & 0 & 0 & 0 & 1 \end{pmatrix}, \quad B := \begin{pmatrix} 1 & -1 & 0 & \dots & 0 \\ -1 & 2 & -1 & \ddots & \vdots \\ 0 & \ddots & \ddots & \ddots & 0 \\ \vdots & \ddots & -1 & 2 & -1 \\ 1 & \dots & 1 & 0 & 2 \end{pmatrix}.$$

This is equivalent to prove that they have the same charateristic polynomial $|A - \lambda I| = |B - \lambda I|$. By summing the first $(N-1)$ first rows to the last one, we obtain

$$|A - \lambda I| = (1-\lambda)|A_{N-1}|, \qquad |B - \lambda I| = (1-\lambda)|B_N|,$$

where $A_{N-1} \in \mathbb{R}^{N-1\times N-1}$ and $B_N \in \mathbb{R}^{N\times N}$ are defined as follows

$$A_{N-1} = \begin{pmatrix} 2-\lambda & -1 & 0 & \dots & 0 \\ -1 & 2-\lambda & -1 & \ddots & \vdots \\ 0 & \ddots & \ddots & \ddots & 0 \\ \vdots & \ddots & -1 & 2-\lambda & -1 \\ 0 & \dots & 0 & -1 & 2-\lambda \end{pmatrix}, \quad B_N = \begin{pmatrix} 1-\lambda & -1 & 0 & \dots & 0 \\ -1 & 2-\lambda & -1 & \ddots & \vdots \\ 0 & \ddots & \ddots & \ddots & 0 \\ \vdots & \ddots & -1 & 2-\lambda & -1 \\ 1 & \dots & 1 & 1 & 1 \end{pmatrix}.$$

The next step consists in stating that

$$|A_{N-1}| = |B_N|, \tag{28}$$

which will be proved recursively. For $N = 3$, it is straightforward to obtain

$$|A_2| = |B_3| = (2-\lambda)^2 - 1.$$

Then, we assume that the property (28) holds true until $N \leq m$ and prove it for $m+1$. Developing $|B_{m+1}|$ with respect to the last column yields

$$|B_{m+1}| = |B'_m| + |B_m|\,,$$

with B'_m and B_m two matrices of $\mathbb{R}^{m\times m}$ defined by

$$B'_m = \begin{pmatrix} 1-\lambda & -1 & 0 & \dots & 0 \\ -1 & 2-\lambda & -1 & \ddots & \vdots \\ 0 & \ddots & \ddots & \ddots & 0 \\ \vdots & \ddots & -1 & 2-\lambda & -1 \\ 0 & \dots & 0 & -1 & 2-\lambda \end{pmatrix}, \quad B_m = \begin{pmatrix} 1-\lambda & -1 & 0 & \dots & 0 \\ -1 & 2-\lambda & -1 & \ddots & \vdots \\ 0 & \ddots & \ddots & \ddots & 0 \\ \vdots & \ddots & -1 & 2-\lambda & -1 \\ 1 & \dots & 1 & 1 & 1 \end{pmatrix}.$$

From (28) we get $|A_{m-1}| = |B_m|$ which provides $|B_{m+1}| = |B'_m| + |A_{m-1}|$. Finally, we note

$$|A_{m-1}| = \begin{vmatrix} 2-\lambda & -1 & 0 & \dots & 0 \\ -1 & 2-\lambda & -1 & \ddots & \vdots \\ 0 & \ddots & \ddots & \ddots & 0 \\ \vdots & \ddots & -1 & 2-\lambda & -1 \\ 0 & \dots & 0 & -1 & 2-\lambda \end{vmatrix}_{m-1\times m-1} = \begin{vmatrix} 1 & 0 & 0 & \dots & 0 \\ -1 & 2-\lambda & -1 & \ddots & \vdots \\ 0 & \ddots & \ddots & \ddots & 0 \\ \vdots & \ddots & -1 & 2-\lambda & -1 \\ 0 & \dots & 0 & -1 & 2-\lambda \end{vmatrix}_{m\times m}$$

which gives

$$|B_{m+1}| = |B'_m| + |A_{m-1}| = \begin{vmatrix} 2-\lambda & -1 & 0 & \dots & 0 \\ -1 & 2-\lambda & -1 & \ddots & \vdots \\ 0 & \ddots & \ddots & \ddots & 0 \\ \vdots & \ddots & -1 & 2-\lambda & -1 \\ 0 & \dots & 0 & -1 & 2-\lambda \end{vmatrix}_{m\times m} = |A_m|\,.$$

The other results are demonstrated using similar arguments. □

B Derivation of the simplified Dynamo model

The Dynamo model originally derived in [5] consists of the set of equations (23) but with the following mobility matrices

$$\mathbb{M}_e = \begin{pmatrix} \mu_e^P & -\mu_e^H & 0 \\ \mu_e^H & \mu_e^P & 0 \\ 0 & 0 & \mu_e^\parallel \end{pmatrix}, \ \mathbb{M}_i = \begin{pmatrix} \mu_i^P & \mu_i^H & 0 \\ -\mu_i^H & \mu_i^P & 0 \\ 0 & 0 & \mu_i^\parallel \end{pmatrix}, \ \mathbb{M} = \begin{pmatrix} \mu^P & -\mu^H & 0 \\ \mu^H & \mu^P & 0 \\ 0 & 0 & \mu^\parallel \end{pmatrix},$$

the so-called field aligned, Pedersen and Hall mobilities for the species α, namely $\mu_\alpha^\parallel$, μ_α^P and μ_α^H, together with the total mobilities, are defined by

$$\begin{aligned} &\mu_\alpha^P = \frac{\kappa_\alpha}{\kappa_\alpha^2 + |B|^2}, \qquad \mu_\alpha^H = \frac{|B|}{\kappa_\alpha^2 + |B|^2}, \quad \mu_\alpha^\parallel = \frac{1}{\kappa_\alpha}, \\ &\mu^P = \mu_e^P + \mu_i^P, \qquad \mu^H = \kappa_e \mu_e^H + \kappa_i \mu_i^H, \quad \mu^\parallel = \mu_e^\parallel + \mu_i^\parallel, \end{aligned} \tag{29}$$

with κ_α the reciprocal of the particle mobility

$$\kappa_\alpha = \frac{m_\alpha \nu_\alpha}{e},$$

where e is the elementary charge, ν_α being the collision frequency of the particles of species α against the neutral which verifies

$$\frac{\nu_e}{\nu_i} = \sqrt{\frac{m_i}{m_e}}. \tag{30}$$

Under the assumption

$$\frac{\kappa_e}{|B|} \sim \varepsilon, \frac{\kappa_i}{|B|} \sim \kappa\varepsilon, \text{ with } \varepsilon \ll 1, \tag{31}$$

the following scaling relations for the Pedersen, Hall and field aligned mobilities hold true

$$\begin{aligned} \mu^P \sim \frac{1}{|B|^2}(\kappa_e + \kappa_i) \sim \kappa\varepsilon, \qquad & \mu^H \sim \frac{1}{|B|^2}\left(\kappa_e^2 - \kappa_i^2\right) \sim \kappa^2\varepsilon^2, \\ \mu_i^P \kappa_i - \mu_e^P \kappa_e \sim \frac{1}{|B|^2}\frac{\kappa_e^2 - \kappa_i^2}{|B|^2} \sim \kappa^2\varepsilon^2, \qquad & \mu_i^H \kappa_i + \mu_e^H \kappa_e \sim \frac{\kappa_i + \kappa_e}{|B|} \sim \kappa\varepsilon, \\ \mu_i^\parallel \kappa_i - \mu_e^\parallel \kappa_e = 0. & \end{aligned}$$

This demonstrates that μ^H can be neglected in front of μ^P in $\mathbb{M}$ while the contribution of μ_α^P may be omitted in $\mathbb{M}_\alpha$, hence the simplified system (23).

References

[1] P. R. Amestoy, I. S. Duff, J.-Y. L'Excellent, and J. Koster. A Fully Asynchronous Multifrontal Solver Using Distributed Dynamic Scheduling. *SIAM Journal on Matrix Analysis and Applications*, 23(1):15–41, Jan. 2001.

[2] P. R. Amestoy, A. Guermouche, and S. Pralet. Hybrid scheduling for the parallel solution of linear systems. *Parallel Computing*, 32:136–156, 2006.

[3] P. Angot, T. Auphan, and O. Gus. Asymptotic-Preserving Methods for an Anisotropic Model of Electrical Potential in a Tokamak. In J. Fuhrmann, M. Ohlberger, and C. Rohde, editors, *Finite Volumes for Complex Applications VII-Elliptic, Parabolic and Hyperbolic Problems*, volume 78, pages 471–478. Springer International Publishing, Cham, 2014.

[4] M. Benzi. Preconditioning Techniques for Large Linear Systems: A Survey. *Journal of Computational Physics*, 182(2):418–477, Nov. 2002.

[5] C. Besse, J. Claudel, P. Degond, F. Deluzet, G. Gallice, and C. Tessieras. A model hierarchy for ionospheric plasma modeling. *Mathematical Models and Methods in Applied Sciences*, 14(3):393416, 2004.

[6] C. Besse, J. Claudel, P. Degond, F. Deluzet, G. Gallice, and C. Tessieras. Instability of the ionospheric plasma: modeling and analysis. *SIAM Journal on Applied Mathematics*, pages 2178–2198, 2005.

[7] C. Besse, J. Claudel, P. Degond, F. Deluzet, G. Gallice, and C. Tessieras. Numerical simulations of the ionospheric striation model in a non-uniform magnetic field. *Computer Physics Communications*, 176(2):75–90, Jan. 2007.

[8] C. Besse, F. Deluzet, C. Negulescu, and C. Yang. Efficient numerical methods for strongly anisotropic elliptic equations. *J Sci Comput*, 55(1):231–254, Apr. 2013.

[9] R. Bridson and W. Tang. Ordering, Anisotropy, and Factored Sparse Approximate Inverses. *SIAM Journal on Scientific Computing*, 21(3):867–882, Jan. 1999.

[10] S. Brull, P. Degond, and F. Deluzet. Degenerate Anisotropic Elliptic Problems and Magnetized Plasma Simulations. *Communications in Computational Physics*, 11(1):147–178, 2012.

[11] S. Brull, P. Degond, F. Deluzet, and A. Mouton. Asymptotic-Preserving scheme for a bi-fluid Euler-Lorentz model. *Kinetic and Related Models*, 4(4):991–1023, Dec. 2011.

[12] S. Brull, F. Deluzet, and A. Mouton. Numerical resolution of an anisotropic non-linear diffusion problem. *Communications in Mathematical Sciences*, 13(1):203–224, 2015.

[13] N. Crouseilles, M. Kuhn, and G. Latu. Comparison of numerical solvers for anisotropic diffusion equations arising in plasma physics. July 2014.

[14] P. Degond. Asymptotic-preserving schemes for fluid models of plasmas. *Panoramas et synthéses of the SMF*, 39-40:1–90, 2013.

[15] P. Degond and F. Deluzet. Asymptotic-Preserving methods and multiscale models for plasma physics. *arXiv:1603.08820 [math-ph, physics:physics], Submitted to Journal of Computational Phy*, Mar. 2016. arXiv: 1603.08820.

[16] P. Degond, F. Deluzet, A. Lozinski, J. Narski, and C. Negulescu. Duality-based asymptotic-preserving method for highly anisotropic diffusion equations. *arXiv:1008.3405*, Aug. 2010.

[17] P. Degond, F. Deluzet, L. Navoret, A.-B. Sun, and M.-H. Vignal. Asymptotic-preserving particle-in-cell method for the vlasovpoisson system near quasineutrality. *Journal of Computational Physics*, 229(16):5630–5652, 2010.

[18] P. Degond, F. Deluzet, and C. Negulescu. An asymptotic preserving scheme for strongly anisotropic elliptic problems. *Multiscale Modeling & Simulation*, 8(2):645–666, 2010.

[19] F. Deluzet, S. Possanner, and M. Ottaviani. The drift limit in the Euler-Lorentz equations via Asymptotic-Preservig numerical simulations. Submitted to Journal of Computational Physics.

[20] F. Filbet, C. Negulescu, and C. Yang. Numerical study of a nonlinear heat equation for plasma physics. *Int. J. Comput. Math.*, 89(8):10601082, May 2012.

[21] P. F. Fischer. Anisotropic diffusion in a toroidal geometry. *Journal of Physics: Conference Series*, 16(1):446, 2005.

[22] J. D. Huba, G. Joyce, and J. Krall. Three-dimensional modeling of equatorial spread f. In M. A. Abdu and D. Pancheva, editors, *Aeronomy of the Earth's Atmosphere and Ionosphere*, number 2 in IAGA Special Sopron Book Series, pages 211–218. Springer Netherlands, Jan. 2011.

[23] J. D. Huba, United States, Office of Naval Research, United States, and Naval Research Laboratory. *2007 plasma formulary: handbook of data and tables for plasma physics and engineering*. Wexford Press, [S.l.], 2007.

[24] S. Jin. Efficient asymptotic-preserving (AP) schemes for some multiscale kinetic equations. *SIAM J. Sci. Comput.*, 21:441454, Sept. 1999. ACM ID: 339309.

[25] S. Jin. Asymptotic preserving (AP) schemes for multiscale kinetic and hyperbolic equations: a review. *Lecture Notes for Summer School on "Methods and Models of Kinetic Theory" June 2010, Rivista di Matematica della Universita di Parma*, pages 177–206, 2012.

[26] M. C. Kelley. *The Earth's Ionosphere, Volume 96, Second Edition: Plasma Physics & Electrodynamics*. Academic Press, 2 edition, June 2009.

[27] M. J. Keskinen. Three-dimensional nonlinear evolution of equatorial ionospheric spread-f bubbles. *Geophysical Research Letters*, 30(16), 2003.

[28] A. Lozinski, J. Narski, and C. Negulescu. Highly anisotropic temperature balance equation and its asymptotic-preserving resolution. *arXiv:1203.6739 [math]*, Mar. 2012. arXiv: 1203.6739.

[29] J. Narski and M. Ottaviani. Asymptotic preserving scheme for strongly anisotropic parabolic equations for arbitrary anisotropy direction. *arXiv:1303.5219 [math]*, Mar. 2013. arXiv: 1303.5219.

[30] A. Ratnani, E. Franck, B. Nkonga, A. Eksaeva, and M. Kazakova. Anisotropic Diffusion in Toroidal geometries. *ESAIM: Proceedings and Surveys*, 53:77–98, Mar. 2016.

[31] Y. Saad. SPARSKIT: A basic tool kit for sparse matrix computations. Technical report, May 1990.

[32] Y. Saad. *Iterative Methods for Sparse Linear Systems, Second Edition*. Society for Industrial and Applied Mathematics, 2 edition, Apr. 2003.

[33] M. Tang and Y. Wang. An asymptotic preserving method for strongly anisotropic diffusion equations based on field line integration. *Journal of Computational Physics*, 330:735–748, 2017.

[34] C. Yang. *Analyse et mise en œuvre des schémas numériques pour la physique des plasmas ionosphériques et de tokamaks*. PhD thesis, Université Lille 1 Sciences et Technologies, Lille, Nov. 2011.

[35] C. Yang and L. M. Tine. A hybrid finite volume method for advection equations and its applications in population dynamics. *to appear in Numerical Methods for Partial Differential Equations*, 2017.